Cerebral Cortex, February 2018;28: 493–509

doi: 10.1093/cercor/bhw384
Advance Access Publication Date: 28 December 2016
Original Article

ORIGINAL ARTICLE

DMRT5 Together with DMRT3 Directly Controls Hippocampus Development and Neocortical Area Map Formation

Sarah De Clercq[1,†], Marc Keruzore[1,†], Elodie Desmaris[1], Charlotte Pollart[1], Stavroula Assimacopoulos[2], Julie Preillon[1], Sabrina Ascenzo[1], Clinton K. Matson[3], Melody Lee[4], Xinsheng Nan[5], Meng Li[5], Yasushi Nakagawa[4], Tino Hochepied[6,7], David Zarkower[3], Elizabeth A. Grove[2] and Eric J. Bellefroid[1]

[1]ULB Institute of Neuroscience (UNI), Université Libre de Bruxelles (ULB), B-6041 Gosselies, Belgium, [2]Department of Neurobiology, University of Chicago, Chicago, IL 60637, USA, [3]Department of Genetics, Cell Biology and Development, Minneapolis, MN 55455, USA, [4]Department of Neuroscience, University of Minnesota, Minneapolis, MN 55455, USA, [5]School of Medicine and School of Bioscience , Neuroscience and Mental Health Research Institute, Cardiff University, Cardiff, CF10 3XQ, UK, [6]Department of Biomedical Molecular Biology, Ghent University, B-9052 Ghent, Belgium and [7]Inflammation Research Center, VIB, B-9052 Ghent, Belgium

Address correspondence to Eric J. Bellefroid, ULB-UNI, Rue des Profs. Jeener et Brachet 12, B-6041 Gosselies, Belgium. Email: ebellefr@ulb.ac.be

[†]These authors contributed equally to this work.

Abstract

Mice that are constitutively null for the zinc finger *doublesex and mab-3 related* (*Dmrt*) gene, *Dmrt5/Dmrta2,* show a variety of patterning abnormalities in the cerebral cortex, including the loss of the cortical hem, a powerful cortical signaling center. In conditional *Dmrt5* gain of function and loss of function mouse models, we generated bidirectional changes in the neocortical area map without affecting the hem. Analysis indicated that DMRT5, independent of the hem, directs the rostral-to-caudal pattern of the neocortical area map. Thus, DMRT5 joins a small number of transcription factors shown to control directly area size and position in the neocortex. *Dmrt5* deletion after hem formation also reduced hippocampal size and shifted the position of the neocortical/paleocortical boundary. *Dmrt3,* like *Dmrt5,* is expressed in a gradient across the cortical primordium. Mice lacking *Dmrt3* show cortical patterning defects akin to but milder than those in *Dmrt5* mutants, perhaps in part because *Dmrt5* expression increases in the absence of *Dmrt3*. DMRT5 upregulates *Dmrt3* expression and negatively regulates its own expression, which may stabilize the level of DMRT5. Together, our findings indicate that finely tuned levels of DMRT5, together with DMRT3, regulate patterning of the cerebral cortex.

Key words: cortical hem, hippocampus, neocortex, neocortical area map, transcription factor

Introduction

Cerebral cortex is divided into 6-layered neocortex, paleocortex or olfactory cortex, and archicortex, comprising the hippocampus and perihippocampal fields. The hippocampus is key to memory, and distinct areas within the neocortex mediate higher functions such as perception, attention, and behavioral planning (Nauta and Feirtag 1986). Genetic defects influencing early cortical development underlie many human neuropsychiatric and neurological disorders (Gaitanis and Walsh 2004; Hu et al. 2014), and, particularly germane to the present study, human DMRTA2/DMRT5 has recently been associated with microcephaly and region-specific neocortical pachygyria (Urquhart et al. 2016).

Embryonic patterning of the cortex begins with the diffusion of signaling molecules from signaling centers (Crossley et al. 2001; Ohkubo et al. 2002; Mangale et al. 2008; Toyoda et al. 2010). Fibroblast growth factors (FGFs) disperse from the rostral telencephalic patterning center (RTPC) (Crossley and Martin 1995; Bachler and Neubuser 2001; Storm et al. 2006; Cholfin and Rubenstein 2007), and WNT and bone morphogenetic proteins (BMPs) from the dorsomedial roof plate and cortical hem (Furuta et al. 1997; Grove et al. 1998). FGFs from the RTPC specify areas of rostral neocortex and establish the rostrocaudal axis of the entire neocortex, whereas the hem is required for development of the hippocampus and caudomedial neocortex and helps position the boundary between neocortex and palecortex (Lee et al. 2000; Fukuchi-Shimogori and Grove 2001; Garel et al. 2003; Yoshida et al. 2006; Cholfin and Rubenstein 2007, 2008; Mangale et al. 2008; Toyoda et al. 2010; Caronia-Brown et al. 2014).

WNT, BMP, and FGF signaling interactively regulate in cortical progenitor cells the expression gradients of several transcription factor genes implicated in cortical patterning. These include the homeobox genes *Lhx2*, *Pax6*, and *Emx2*, and the zinc finger *doublesex and mab-3 related* (*Dmrt*) gene, *Dmrt5/Dmrta2* (Monuki et al. 2001; Muzio et al. 2005; Cholfin and Rubenstein 2008; Konno et al. 2012; Saulnier et al. 2013; Caronia-Brown et al. 2014). *Lhx2* has several functions in cortical patterning, first as a selector gene specifying cortical identity (Mangale et al. 2008) and subsequently determining the division between neocortex and paleocortex (Chou et al. 2009). Still later in corticogenesis, *Lhx2* is required for normal development of primary somatosensory cortex (S1) (Shetty et al. 2013). *Pax6* is expressed in a rostrolateral high to caudomedial low gradient in the cortical primordium (CP) and promotes development of rostral areas at the expense of caudal areas (Bishop 2000; Muzio et al. 2002), possibly by differentially regulating cell division along the rostral-to-caudal axis (Gotz et al. 1998; Manuel et al. 2007; Asami et al. 2011; Mi et al. 2013). Additionally, *Pax6* contributes to the development of a normally sized S1 (Zembrzycki et al. 2013). *Emx2* is expressed in an opposite caudomedial high to rostrolateral low gradient and, consistent with this gradient, regulates the size of the hippocampus and caudomedial neocortex (Yoshida et al. 1997; Mallamaci et al. 2000; Tole et al. 2000; Hamasaki et al. 2004; Muzio et al. 2005). To date, whether *Dmrt5*, expressed in the same gradient as *Emx2*, directly plays a similar role is unclear.

In mice constitutively lacking *Dmrt5*, the hippocampus is missing, caudomedial neocortex is extremely reduced, and paleocortex expands dorsally. Additionally, in $Dmrt5^{-/-}$ mice, the cortical hem is virtually gone, suggesting that *Dmrt5* controls cortical patterning indirectly by promoting cortical hem formation (Konno et al. 2012; Saulnier et al. 2013). Yet, *Dmrt5* expression is upregulated by WNT signaling and downregulated by FGF8 (Konno et al. 2012; Saulnier et al. 2013; Caronia-Brown et al. 2014), implying that DMRT5 may also have a second direct role in cortical patterning. It remains unknown therefore, whether DMRT5 itself influences the neocortical area map and whether different levels of DMRT5, induced experimentally, would affect the area map in a "dose-dependent" manner, as is true for EMX2 (Hamasaki et al. 2004; Zembrzycki et al. 2015).

To gain a better understanding of DMRT5's mode of action in cortical development, we generated mice with floxed *Dmrt5* and mated them with mice carrying different Cre alleles. In all cases, the stage of *Dmrt5* deletion followed the initial formation of the cortical hem, just after mid-gestation. In both *Nestin-Cre* and *Emx1-Cre* cKO mice, *Dmrt5* was deleted in the CP. In *Nestin-Cre* cKO animals, however, DMRT5 remained in the cortical hem, whereas it was diminished in *Emx1-Cre* cKO mice. To delete *Dmrt5* from the hem only, *Dmrt5* floxed mice were mated with *Wnt3a-Cre* mice. Comparing the phenotypes of the progeny revealed that at this developmental stage, hippocampal development and neocortical patterning requires DMRT5 in the CP but not in the hem.

For conditional gain of function of *Dmrt5*, we generated a transgenic line that, when crossed with *Emx1-Cre* mice, generated progeny with excess *Dmrt5* expression in the CP. Altering the distribution and levels of DMRT5 led us to conclude that 1) DMRT5 controls patterning of the caudal cortex independent of its influence on the hem, 2) size and position of neocortical areas is sensitive to different levels of DMRT5, and 3) DMRT5 negatively controls *Dmrt5* expression suggesting negative autoregulation.

Finally, we examined the genetic association of *Dmrt5* with *Dmrt3*, related genes that have comparable expression gradients in cortical progenitor cells. *Dmrt3* null mice show cortical defects, but these are much milder than in the *Dmrt5* null. We tested interactions between the *Dmrt* genes by assessing their expression in *Dmrt3* and *Dmrt5* mutant lines. Expression of *Dmrt5* increases in the absence of *Dmrt3*, possibly explaining the more modest cortical phenotype in the *Dmrt3* null and demonstrating that *Dmrt5* expression is negatively controlled not only by DMRT5 but also by the related transcription factor DMRT3.

Materials and Methods

Mouse Lines and Genotyping

All animals were maintained in a C57Bl/6 background except for CD1 mice used for in utero electroporation studies. Midday of the day of vaginal plug discovery was termed embryonic day 0.5 (E0.5), and the first 24 h after birth was P0. Animal care was in accordance with institutional guidelines, and the policies of the US National Institutes of Health.

The *Dmrt5* conditional knockout allele (Supplementary Fig. 1A) was generated using standard recombineering methods. A bacterial artificial chromosome containing the *Dmrt5* gene as well as linearized plasmid DNA containing short *Dmrt5* flanking sequences were electroporated into *Escherichia coli* induced to express homologous recombination machinery. Homologous recombination generated a plasmid containing 11 kb of the mouse *Dmrt5* locus encompassing exons 1–3. Next, *loxP* sites were inserted in this plasmid by homologous recombination into the first and second introns of *Dmrt5* together with a neomycin resistance gene (Neo^R). This plasmid was linearized and electroporated into mouse ES cells to generate the *Dmrt5* conditional mutant allele. ES cells containing the *Dmrt5* conditional knockout allele were provided to the University of Minnesota Mouse Genetics Laboratory for the generation of chimeric mice. Highly chimeric mice were bred to wild-type females. To remove the Neo^R gene from the *Dmrt5* locus, mice containing

the *Dmrt5* conditional knockout allele were bred to mice containing a ubiquitously expressed FlpE recombinase enzyme. This generated mice carrying the final $Dmrt5^{floxed(fl)}$ allele (Supplementary Fig. 1A). $Dmrt5^{fl/fl}$ mice were crossed to *Emx1-IRES-Cre* (Gorski et al., 2002), *Nestin-Cre* (Tronche et al. 1999), or *Wnt3a-IRES-Cre* mice (Yoshida et al. 2006). To distinguish between the wild-type and *Dmrt5* floxed alleles, mice were genotyped by PCR using genomic DNA from the tail and primers: Fwd 5′-TCTCTGTAATCTGAGTCCCTTTCAGG-3′; Rev 5′-GTAC TTCTCCGCTGCCCTCAAC-3′ (Supplementary Fig. 1A, primers a, b "Dmrt5 Lox"). To detect the Cre-excised allele, mice were genotyped by PCR using the following primers on genomic DNA from dorsal telencephalon: Fwd 5′-TCTCTGTAATCTGAGTCCC TTTCAGG-3′; Rev 5′-AGGAAAGGAATCTTGCTGAGAAACG-3′ (Supplementary Fig. 1A, primers a, c "Dmrt5 Δ2").

To generate *Dmrt3* null mutants, we constructed a targeting vector in which exon 1 of *Dmrt3* was replaced by Neo^R flanked by *loxP* sites. After isolation of homologous recombinants in ES cells, the clones were used to generate chimeric mice that were mated to WT mice to generate heterozygous animals. The Neo^R cassette was removed by crossing the $Dmrt3^{neo/+}$ heterozygous mice with *beta-actin Cre* mice. For genotyping, primers used were: Fwd (WT) 5′-ATGAACGGCTACGGCTCCCCCTAC-3′; Fwd (KO) 5′ GGAAAGCGGTCTAGGGCTCAGTGC-3′; Rev 5′-CCCGGGG AAAGCCTCTGACGATAG-3′ (Supplementary Fig. 1B).

For *Dmrt5* gain of function, a *Dmrt5* conditional transgenic mouse model was generated using the Gateway-compatible *ROSA26* locus targeting vector as previously described (Nyabi et al. 2009). The DNA coding sequence corresponding to *Dmrt5* was isolated from pFLCI EST clone: B130012I23. The *Dmrt5* transgene was targeted to the *ROSA26* locus, downstream of a floxed cassette containing a neomycin resistance marker and a transcriptional stop element. To tag transgene-expressing cells with eGFP, an IRES-eGFP element was inserted at the C-terminus of the transgene (Nyabi et al. 2009) (Supplementary Fig. 1C). To distinguish between the wild-type and *Dmrt5* transgene allele, mice were genotyped by PCR using primers: Fwd Rosa26 5′-AAACTGGCCCTTGCCATTGG-3′; Fwd eGFP 5′-AAC GAGAAGCGCGATCACAT-3′; Rev Rosa26 5′-GTCTTTAATCTACC TCGATGG-3′ (Supplementary Fig. 1C, primers d, f, g "Dmrt5Tg").

To distinguish between the floxed targeted allele ($Dmrt5^{Tg}$) and the Cre-excised allele, the following primers were used: Fwd Rosa26 5′-AAACTGGCCCTTGCCATTGG-3′; Rev Neo 5′-CTCGTCC TGCAGTTCATTCA-3′; Rev Dmrt5 5′-TGCCTGCGCAAGGCCACC TGA-3′ (Supplementary Fig. 1C, primers d, e, h "Dmrt5ΔNeo"). In both cases, the presence of Cre recombinase was assessed with primers: Fwd 5′-GTTCGCAAGAACCTGATGGA-3′; Rev 5′-CCACC GTCAGTACGTGAGAT-3′. Crossing *Dmrt5* conditional transgenics (termed here *Dmrt5Tg* mice) with *Emx1-Cre* mice induced in the dorsal telencephalon both eGFP fluorescence and excess DMRT5 protein (Supplementary Fig. 1D,E).

Generation of DMRT5 Antibodies

Polyclonal antibodies for mouse DMRT5 were generated by immunizing rabbits with the 2 following peptides: GRPDSPQPPPGKPLSP DGADSGPRC (aa 200-223) and CKEPGYGGGLYGPMVNGTPEKQ (aa 511-531) (PSL Peptide Specialty Laboratories, GmbH).

Histology and Immunofluorescence

Standard hematoxylin and eosin (H&E) staining was performed on 6–8 μm sections of embryos or brains fixed overnight in 4% paraformaldehyde/PBS, dehydrated and paraffin-embedded. For immunofluorescence, embryos were fixed overnight in 4% paraformaldehyde/PBS, infused in 30% sucrose/PBS overnight, frozen in gelatin (7.5% gelatin, 15% sucrose/PBS) and sectioned in 20 μm cryostat sections. Antigen retrieval was performed by boiling the sections in Target Retrieval Solution Citrate pH 6.0 (DAKO). Sections were then permeabilized in 0.3% Triton X-100 and blocked in 10% goat serum. Primary antibodies used were: DMRT5 (rabbit, 1/2000, gift from Dr Meng Li, Cardiff), CTIP2 (rat, 1/250, abcam ab18465), PAX6 (mouse 1/100, DSHB), β-TUBULIN (mouse, 1/100, Covalent). Secondary antibodies used were: Alexa Fluor 488 goat anti-rabbit (1/400, A-11008, Invitrogen), Alexa Fluor 594 goat anti-mouse (1/400 A11005, Invitrogen) and Alexa Fluor 594 anti-rat (1/400, A11007, Invitrogen). Sections were counterstained with DAPI. Wide-field images were acquired with a Axio Observer Z1 microscope.

In Situ Hybridization

In situ hybridization (ISH) on sections was performed using antisense digoxigenin-labeled riboprobes as described (Saulnier et al. 2013). *Dmrt5* expression in *Emx1* cKO embryos and in *Dmrt3* KO embryos were analysed using an antisense probe corresponding to the 3′ half of exon three synthetized by linearizing EST AI592924 (Genbank) with EcoRI and transcribing it with T3 as previously described (Saulnier et al. 2013). Endogenous *Dmrt5* expression in *Dmrt5Tg* mutants was evaluated using an antisense probe corresponding to a portion of the 3′ UTR generated by linearizing the same EST with BamHI and transcribing it with T3. The other antisense probes were generated from the following previously described cDNA clones: *Lmo3*, *Lmo4* (Bulchand et al. 2001), *Cdh6* (Bishop 2000), and *tdTomato* (Genove et al. 2005). For whole-mount ISH, brains stored in methanol 100% were rehydrated and treated with a 6% hydrogen peroxide solution for 60 min. Brains were then incubated with 20 μg/ml proteinase K for 45 min (E18.5) or 55 min (P7) and post-fixed 20 min in 4% paraformaldehyde/0,2% gluteraldehyde. Brains were incubated in hybridization solution (50% formamide, 5X SSC, 10% (E18.5) or 20% (P7) SDS, 500 μg/ml tRNA, 200 μg/ml acetylated BSA, 50 μg/ml heparin) for at least 1h at 70°C, then hybridized to digoxigenin-labeled riboprobes (1–2 μg/mL) in hybridization solution overnight at 70 °C. The next day, brains were washed in solution X (50% formamide, 2X SSC, 1% SDS) 4 × 45 min at 70 °C and equilibrated in MABT (0.1 M maleic acid, 150 mM NaCl, 1% Tween-20, pH 7.5) 3 × 10 min. Brains were then blocked 2 h in blocking solution (10% lamb serum, 2% blocking reagent (Roche) in MABT) and incubated with anti-digoxigenin antibody (1/4000, Roche) in blocking solution overnight at 4 °C. The next day, brains were washed at least 5 × 1 h and then overnight in MABT. Finally, brains were incubated 3 × 10 min in NTMT (100 mM NaCl, 100 mM Tris-HCl pH 9.5, 50 mM $MgCl_2$, 1% Tween-20, 2 mM Levamisole) and detection of the anti-digoxigenin antibody was performed by NBT/BCIP solution at room temperature. Images were acquired with an Olympus SZX16 stereomicroscope and an Olympus XC50 camera, using the Imaging software Cell*.

Quantification of the dorsal surface area of the cortical hemisphere of E12.5, E18.5, P7, and adult animals was obtained by taking measurements from images of whole brains. Measurement of the surface areas of primary motor, sensorimotor, and visual neocortex, M1, S1, and V1 in P7 brains were obtained by outlining the corresponding regions with specific probes as indicated in the text and taking measurements from images of whole brains as above. The results are presented as the ratio of the M1, S1, and V1 areas relative to the total dorsal surface area of the cortex. Photographs were taken with an Olympus SZX16

stereomicroscope. Measurements were done using the Imaging software Cell*. All quantified data are expressed as mean values ± standard deviation (SD). Significance tests were performed using a 2-tailed Student's *t-test*; *P*-values less than 0.05 were regarded as statistically significant. Each experiment was repeated on at least 4 biological samples for each genotype.

RNA Isolation and RT-qPCR

Total RNA was extracted from dorsal telencephalon of E12.5 or 14.5 embryos using the RNeasy Mini Kit (Qiagen) according to the manufacturer's protocol. cDNA was synthesized starting from 1 or 2 µg total RNA. RT-qPCRs were performed using a StepOnePlus Real-Time PCR system (Applied Biosystems), GoTaq qPCR Master Mix (Promega) and a program optimized by the manufacturer. Gene expression normalization and primers validation were performed as previously described (Saulnier et al. 2013). Endogenous *Dmrt5* expression in *Dmrt5Tg* mice was analysed using previously described primers (Fwd 5′-GCGTG CTGCGCCAACAGAGG-3′ and Rev 5′-GTGGTCCCGTCGCTGTCG CT-3′) located in exon 1, excluded from the targeting vector, and exon 2, respectively (Saulnier et al. 2013). Transgenic *Dmrt5* expression was evaluated using primers located in the GFP coding sequence inserted downstream of *Dmrt5* in the targeting vector: Fwd 5′-ACGTAAACGGCCACAAGTTC-3′, Rev 5′-AAGTCGTGCTG CTTCATGTG-3′. *Dmrt5* expression in *Emx1-Cre* cKO embryos was analysed using the following primers located in predicted exon 1: Fwd 5′-TGTCTAATGGAGCCCTGAGG-3′, Rev 5′-GAACTT CCGGACCCCTCTAG-3′ (Genbank XM_006503093.3). Primers for *Dmrt3*, *Dmrt4*, *Emx2*, *Lhx2*, *Pax6* (Saulnier et al. 2013), and *Lef1* (Sohn et al. 2012) have been previously described (Saulnier et al. 2013). The other primers used are as follows: *Axin2* Fwd 5′-CCGACCTCAAGTGCAAACTC-3′, *Axin2* Rev 5′-ACATAGCCGG AACCTACGTG-3′; *Bmp4* Fwd 5′-GAGGGATCTTTACCGGCTCC-3′, *Bmp4* Rev 5′-GTTGAAGAGGAAACGAAAAGCAG-3′ (sequences given by Dr E. Monuki, Irvine); *Wnt3a* Fwd 5′-CAGGAACTACG TGGAGATCATGC-3′, *Wnt3a* Rev 5′-CATGGACAAAGGCTGA CTCC-3′. For RT-qPCR analyses, results were normalized to the level of expression in wild-type forebrain. Error bars show SD of 3 independent experiments.

In Utero Electroporation

cDNAs encoding DMRT5 or tdTomato (Genove et al. 2005) were cloned into the pEFX expression vector (Agarwala et al. 2001). The CP was electroporated at E10.5, and brains were collected at E12.5 (Assimacopoulos et al. 2012). *Dmrt5*- and *tdTomato*-containing plasmids were electroporated together so that the electroporation site could be imaged by tdTomato fluorescence immediately after collection of the brains. Brains with appropriately positioned dense electroporation sites were selected as previously described (Toyoda et al. 2010). After sectioning, one series of sections was processed with ISH for *tdTomato* to mark the site of *tdTomato*/*Dmrt5* co-electroporation. This gave a sharper outline of the site than ISH for *Dmrt5* itself, given that *Dmrt5* is normally expressed throughout the CP at these ages. Other series of sections from the same brain were processed with ISH to show up- or downregulation of genes of interest. More than 10 brains with appropriate electroporation sites were processed to show expression of each gene of interest in the experimental and control (tdTomato electroporation only) conditions.

Western Blotting Analysis

E12.5 dorsal telencephalon samples containing each tissue from 2 embryos were dissolved in RIPA buffer (NaCl 150 mM, NP-40 1%, Sodium deoxycholate 0.5%, SDS 0.1%, Tris 50 mM pH 8) containing phosphatase (Sigma) and protease (Roche) inhibitors. The samples were sonicated 2 times 5 s. The protein concentration was determined by Bradford assay (OD 595 nm). Of note, 15 µg of each samples were fractionated by SDS-PAGE and transferred to an Immobilon-FL membrane (Millipore), which was incubated with anti-GAPDH (Mouse, 1/10 000, Sigma) and anti-DMRT5 (Rabbit, 1/10 000) antibodies. The secondary antibodies used were anti-rabbit (1/15 000, IR Dye 800CW, and Li-COR) and anti-mouse (1/15 000, IR Dye 680 RD, Li-COR). The detection and quantification were performed using Odyssey Fc (Li-COR) with the Image Studio software.

Results

A Normal Cortical Hem but Reduced Cortical Hemisphere Size in *Dmrt5* cKO Mice

To determine whether DMRT5 regulates cortical patterning independent of its influence on the cortical hem, $Dmrt5^{Floxed}$ mice ($Dmrt5^{fl/fl}$) were crossed with *Nestin-Cre*, *Wnt3a-Cre*, and *Emx1-Cre* mice to generate conditional *Dmrt5* knockout mice (cKO mice). Key to this study, this set of cKO mice provided both overlapping and complementary patterns of *Dmrt5* deletion. By E12.5, little or no DMRT5 was detected by immunofluorescence (IFl) in the CP of *Nestin-Cre* cKO mice, but strong DMRT5-IFl remained in the hem and developing choroid plexus. By contrast, *Wnt3a-Cre* cKO mice, which initiate recombination before E10 (Yoshida et al. 2006), lacked DMRT5-IFl in the hem but displayed DMRT-IFl equivalent to control levels in the CP and choroid plexus (Fig. 1A). In the E12.5 *Emx1-Cre* cKO mice, DMRT5-IFl was virtually lost in both the hem and CP. Important to this study, deletion of *Dmrt5* in the CP began about a day earlier in *Emx1-Cre* cKO than in *Nestin-Cre* cKO mice, consistent with previous observations (Tronche et al. 1999; Gorski et al. 2002; Sahara and O'Leary 2009). We found that DMRT5-IFl was already greatly reduced in the *Emx1-Cre* cKO CP at E10.5 but remained strong in *Nestin-Cre* cKO mice. By E12.5, however, efficient *Dmrt5* inactivation was evident in the dorsal telencephalon in both *Emx1-Cre* cKO and *Nestin-Cre* cKO lines (Fig. 1A,B and Supplementary Fig.1A).

At E12.5, the cerebral hemispheres were reduced in size in *Emx1-Cre* cKO (−19.3 ± 7.2%, $n = 7$) and *Nestin-Cre* cKO mice (−14.2 ± 7.7%, $n = 8$) (Fig. 1C). The hemispheres in E18.5 and adult *Dmrt5* cKO mice showed slightly greater reduction (E18.5 *Emx1-Cre* cKO: −20.7 ± 4.0%, $n = 12$; E18.5 *Nestin-Cre* cKO: −19.9 ± 5.9%, $n = 7$; adult *Emx1-Cre* cKO: −28.1 ± 11.2%, $n = 3$; adult *Nestin-Cre* cKO: −21.7 ± 8.6%, $n = 4$). The cortical hemispheres in *Emx1-Cre* cKO and *Nestin-Cre* cKO mice were therefore roughly 20% smaller than control hemispheres, a much less severe reduction than observed in constitutively null *Dmrt5* mice at E18.5 (Saulnier et al. 2013). The cortical hemispheres in *Wnt3a-Cre* cKO and control mice were indistinguishable in size at both E12.5 and E18.5 ($n = 7$ and 10/genotype, respectively) (Fig. 1C).

Dmrt5 constitutively null embryos show dramatic reduction of *Wnt* gene expression and WNT signaling activity at the cortical hem (Konno et al. 2012; Saulnier et al. 2013). By contrast, RT-qPCR and section ISH revealed that genes encoding components of the WNT pathway were expressed virtually normally

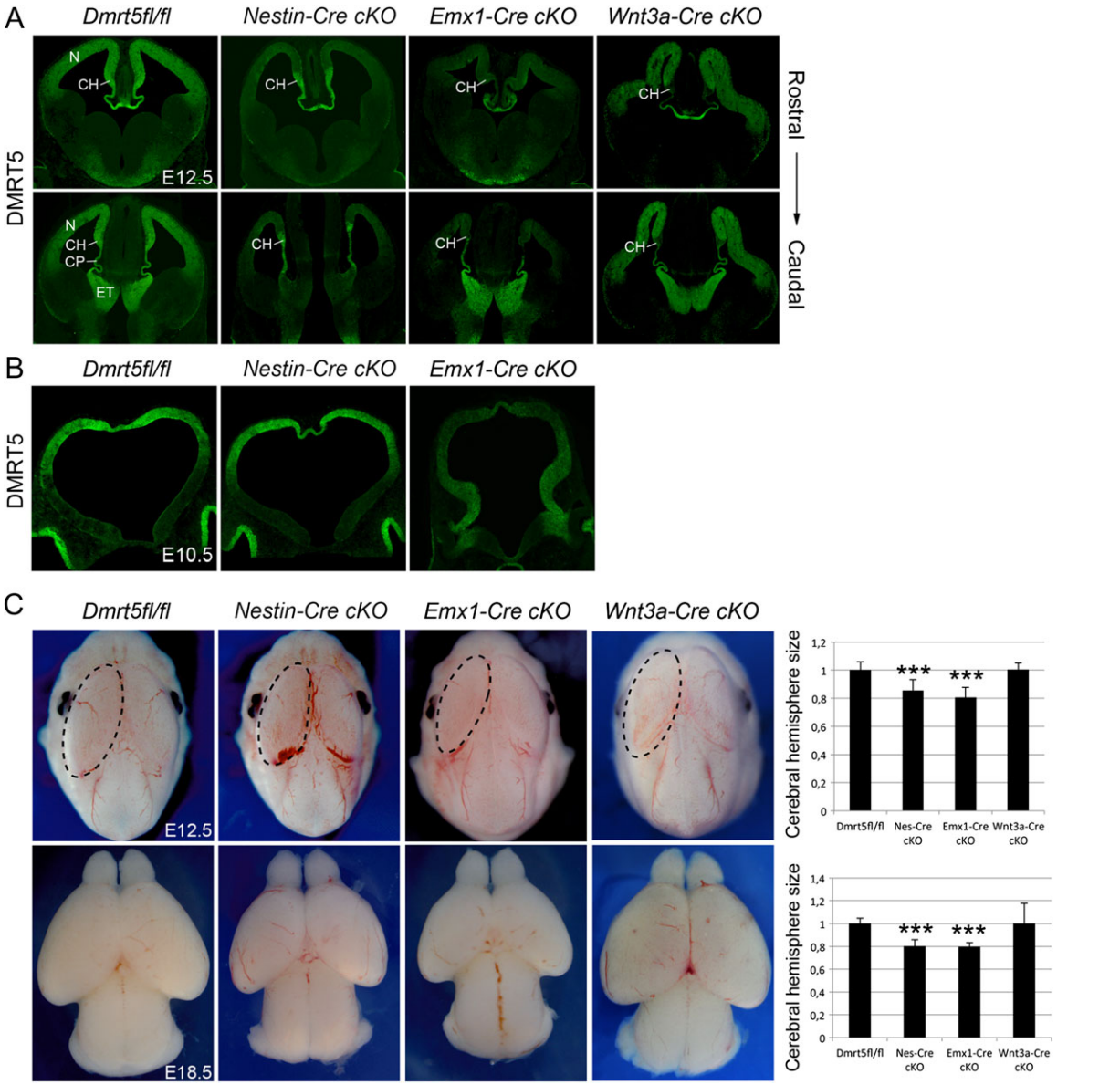

Figure 1. Cerebral hemispheres are reduced in *Dmrt5 Emx1-Cre* and *Nestin-Cre* cKO brains but not in *Wnt3a-Cre* cKO mice. (*A*, left to right) Coronal sections through E12.5 brains. Normal DMRT5-IFl in control mice; *Nestin-Cre* cKO retains DMRT5-IFl in the cortical hem and choroid plexus but not in the CP; *Emx1-Cre* cKO loses DMRT-IFl in both the hem and CP and *Wnt3a-Cre* cKO loses DMRT-IFl only in the hem. CP, choroid plexus; ET, eminentia thalami; CH, cortical hem; N, neocortex. (*B*) DMRT5-IFl on coronal sections through E10.5 brains. DMRT5-IFl is already reduced in the cortex of *Emx1-Cre* mice but is near control levels in *Nestin-Cre* mice. (*C*) Dorsal views of E12.5 and E18.5 control and *Dmrt5* cKO brains. Graphs representing the surface area of *Dmrt5* cKO cerebral hemispheres compared to controls are shown on the right (***$P < 0.001$).

in *Nestin-Cre*, *Emx1-Cre*, and even *Wnt3a-Cre* cKO mice, in which *Dmrt5* was deleted specifically in the hem (Supplementary Fig. 2). No significant differences were seen between *Dmrt5* cKO mice and control animals in expression levels within the hem of *Wnt3a*, the earliest *Wnt* gene expressed selectively in this region (Lee et al. 2000), *Lef1*, a Wnt nuclear effector, *Axin2*, a highly reliable indicator of canonical WNT activity, and *Bmp4* in the choroid plexus and ventral hem (Furuta et al. 1997; Grove et al. 1998; Ma et al. 2002; Muzio et al. 2005). Domains of *Lef1* and *Axin2* expression appear, however, slightly smaller in *Emx1-Cre* cKOs compared with control mice, reflecting the strongly reduced hippocampal primordium (Supplementary Fig. 2A, and see below). In summary, *Dmrt5* cKO mice have a cortical hem that appears normal by morphology and gene expression, indicating that severe hem defects in the *Dmrt5* null are caused by loss of DMRT5 very early in embryogenesis. We next identified cortical deficits in *Dmrt5* cKO mice that persisted despite the presence of the hem.

Hippocampal Fields Are Reduced in *Emx1-Cre* and *Nes-Cre* but not in *Wnt3a-Cre cKO* Mice

At E18.5, the hippocampus was markedly reduced in *Nestin-Cre* cKO and *Emx1-Cre* cKO mice, but not in *Wnt3a-Cre* cKO mice (Fig. 2A). At E18.5, no morphological dentate gyrus (DG) could be identified in H&E-stained coronal sections from *Nestin-Cre* cKO or *Emx1-Cre* cKO brains (Fig. 3A). Hippocampal field-specific gene

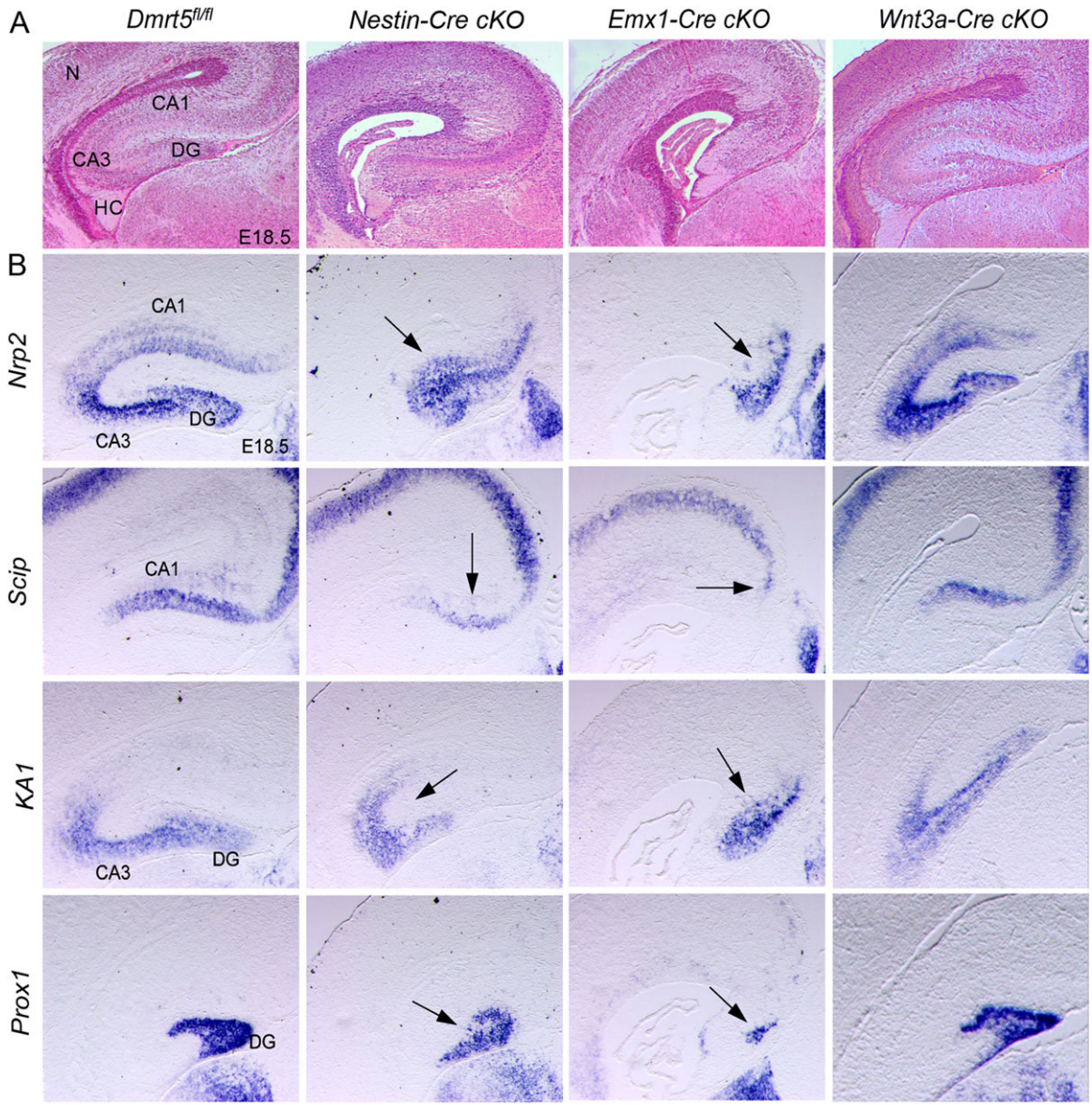

Figure 2. Hippocampus is reduced after conditional loss of *Dmrt5* in the CP. (*A*) H&E-stained coronal brain sections at E18.5. The hippocampus is reduced in *Nestin-Cre* cKO and severely diminished in *Emx1-Cre* cKO mice (compare with control mouse, far left). In *Wnt3a-Cre* cKO, in which *Dmrt5* is lost only from the hem, the hippocampus resembles the control. (*B*) Coronal sections through E18.5 brains processed by ISH. All hippocampal fields including the DG are present in cKO mice but smaller in *Nestin-Cre* and *Emx1-Cre* cKO animals (arrows). In contrast, individual fields in the *Wnt3a-Cre* cKO resemble those in the control mouse. HC, hippocampal commissure; N, neocortex.

expression (*Nrp2, Scip/Pou3f1, KA1/Grik4*, and *Prox1*) revealed that hippocampal fields, including the DG, were present but much smaller than normal in *Nestin-Cre* cKO and *Emx1-Cre* cKO mice. In *Wnt3a-Cre* cKO mice, in contrast, the hippocampus and hippocampal fields resembled those in control mice (Fig. 2*B*). The decrease in hippocampal field size was more severe in *Emx1-Cre* than *Nestin-Cre* cKO embryos, but less so than in *Dmrt5* null mice in which the hippocampus is almost completely lost (Konno et al. 2012; Saulnier et al. 2013). Thus, the severity of the hippocampal defect correlated with the time of *Dmrt5* deletion in the CP given that *Emx1-Cre* drives recombination about a day earlier than *Nestin-Cre*. In summary, while signals from the cortical hem are necessary and sufficient for the hippocampus to form (Mangale et al. 2008), DMRT5 is required in the CP, the responsive tissue, for normal hippocampal development.

Emx1-Cre cKO but not *Nes-Cre* cKO Mice Display Changes in Dorsoventral Cortical Patterning

In the absence of the cortical hem, dorsomedial neocortex is reduced and ventrolateral olfactory cortex, or paleocortex, expands, not only proportional to the smaller hemisphere of the hem-ablated mouse but also in absolute size relative to control mice (Furuta et al. 1997). A similar shift was previously reported in the *Dmrt5* constitutively null mouse (Saulnier et al. 2013) and in the present study was observed in *Emx1-Cre* cKO mice. *Nrp2*, encoding a neuropilin receptor, is expressed in paleocortex (Chen et al. 1997; Caronia-Brown et al. 2014). In whole-mount brains and cortical tissue sections processed for ISH at E18.5, *Nrp2* expression indicated a larger dorsal extent of the olfactory cortex, in

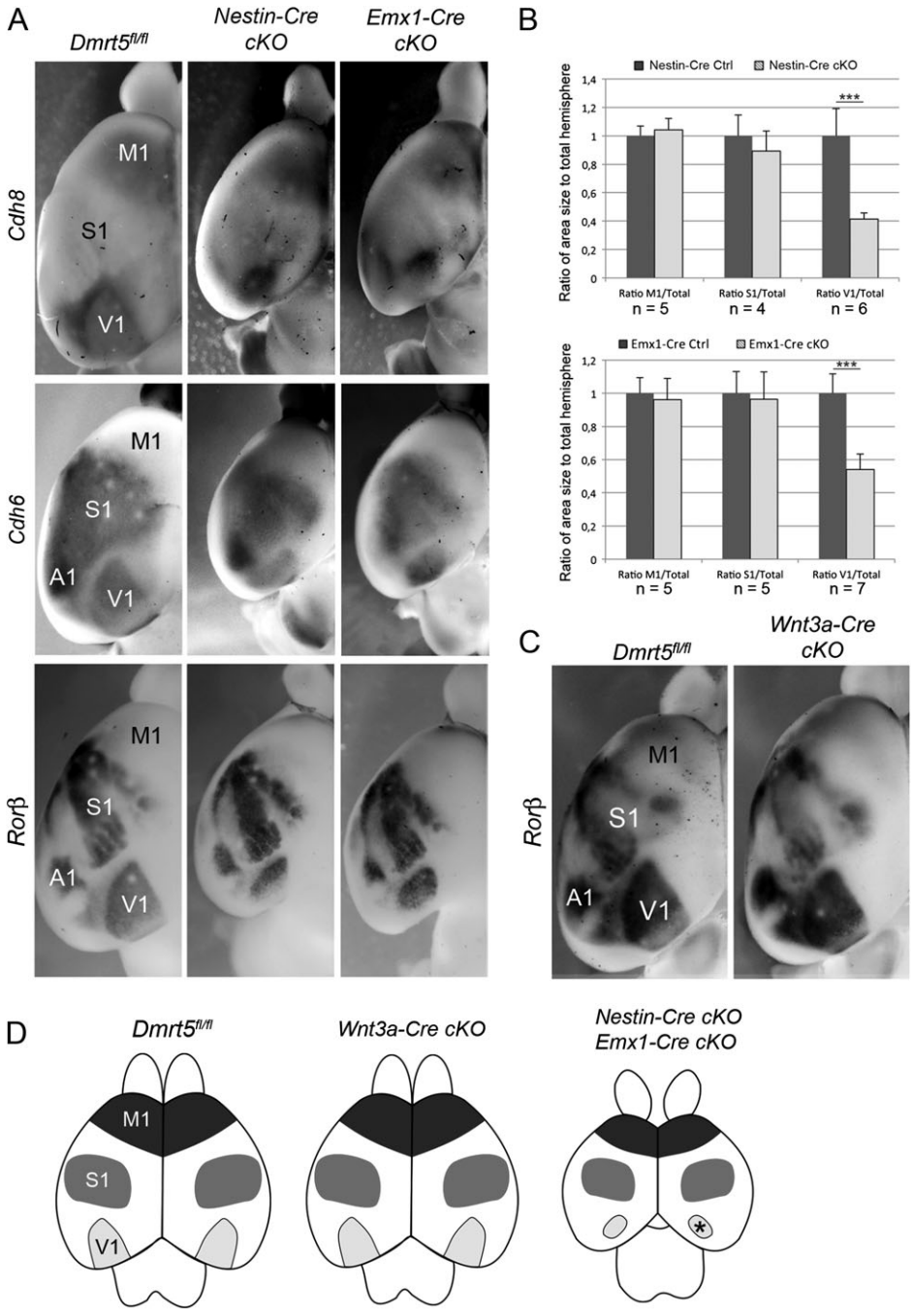

Figure 3. Extreme reduction of V1 with conditional deletion of *Dmrt5* in the CP. (*A*) Dorsal views of P7 whole-mount brains processed with ISH for *Cdh6*, *Cdh8*, or *Rorβ* to outline neocortical areas. In *Nestin-Cre* and *Emx1-Cre* cKO brains, the cortical hemispheres are smaller than in control brains, and V1 areas appear minute. In control mice, moderate expression of all three genes outline the triangular area of V1; stronger expression of *Cdh8* indicates higher order visual areas surrounding V1. (*B*) As a ratio of surface area to total hemisphere size, V1 in both cKO mice is significantly reduced (***P < 0.001), S1 and M1 are not significantly different from controls, *n* = number of samples examined. (*C*) Control and *Wnt3a-Cre* cKO hemispheres are indistinguishable in overall size and in the sizes of *Rorβ*-expressing S1, A1, and V1. (*D*) Schematic representation of the primary M, S, and V area size observed in the neocortex of the different *Dmrt5* cKO mice. Reduced V1 size in *Nestin-Cre* and *Emx1-Cre* cKOs is indicated by an asterisk.

absolute size, compared with control and *Nestin-Cre* cKO mice (Supplementary Fig. 3A,B). In a complementary pattern, expression of *Scip/Pou3f1* marked a notably reduced dorsomedial neocortex in the *Emx1-Cre* cKO mutants (Supplementary Fig. 3C). Expression of *CTIP2* in layer V neurons in the neocortex continues ventrally into layer II of piriform cortex, thereby forming a broken band of expression. The position of the break in *CTIP2* expression in *Emx1*-Cre cKO mice further indicated the greater dorsal extent of olfactory cortex (Supplementary Fig. 3D). Finally, *Lmo3* expression illustrated the expansion at E18.5 and P7 (Supplementary Fig. 3E). Relatively little is known about the mechanisms that separate neocortex and paleocortex, except that the transcription factor LHX2 is critical (Chou et al. 2009). Our observations

suggest that DMRT5 helps position the boundary between the two types of cortex, and, similar to LHX2, is required earlier than E11.5, before substantial cortical neurogenesis.

Caudomedial Neocortical Areas are Reduced in Emx1-Cre and Nestin-Cre cKO Mice but not in Wnt3a-Cre cKOs

In constitutively *Dmrt5* null mouse, the caudomedial neocortex is strongly reduced (Konno et al. 2012; Saulnier et al. 2013). The *Dmrt5* null mice rarely survive past birth, preventing identification of the neocortical areas involved. *Nestin-Cre* cKO and *Emx1-Cre* cKO mice live on, and at the end of the first postnatal week, area boundaries can be identified by the expression patterns of several genes, including *Cdh6, Cdh8, Lmo4*, and *Rorβ* (Assimacopoulos et al. 2012). At postnatal day 7 (P7), V1 is distinguished as a domain of moderate *Cdh8* expression, surrounded by stronger *Cdh8* expression in higher order visual areas. *Cdh8* is also expressed in a frontal region that includes the primary motor area (M1) (Fig 3A, $Dmrt5^{fl/fl}$). Strong to moderate *Cdh6* and *Rorβ* expression demarcates V1, and primary somatosensory (S1) and auditory (A1) areas; weaker *Rorβ* expression appears in some higher order visual areas (Fig. 3A, $Dmrt5^{fl/fl}$).

The area of a cortical hemisphere in dorsal view at P7 was about 70% of control size in *Nestin-Cre* (71.5 ± 5%, $n = 5$ litters) and *Emx1-Cre* (71.6 ± 3.3%, $n = 5$ litters) cKO brains. *Wnt3a-Cre* cKO hemispheres were the same size as in control brains (102 ± 4%, $n = 3$ litters). In both *Nestin-Cre* and *Emx1-Cre* cKO whole-mount brains, processed for ISH at P7, the caudomedial area V1 was greatly reduced (Fig. 3A). Changes in the surface areas of V1, S1, and M1 were quantified by determining the ratio of each, demarcated by expression of gene expression markers, versus the total hemisphere surface area. In *Emx1-Cre* cKO and *Nestin-Cre* cKO mice, the ratio of the area of V1 to the total hemisphere surface area was roughly half that in control mice, confirming a disproportionate reduction, whereas the ratios of M1 and S1 to total surface area in cKO mice were not significantly different from controls (Fig. 3B). In *Wnt3a-Cre cKO* mice, the area map outlined by *Rorβ* expression was indistinguishable from that of control mice (Fig. 3C). These observations (summarized in Fig. 3D) suggest that DMRT5 in neocortical progenitor cells regulates the position and size of V1 and presumably other caudomedial neocortical areas. The smaller overall size of the cortical hemispheres in *Emx1-Cre* cKO and *Nestin-Cre* cKO mice compared with controls, however, raises the alternative possibility that loss of *Dmrt5* causes both general and region-specific tissue loss that is more evident in the caudomedial region where *Dmrt5* expression is highest.

Overexpression of DMRT5 Expands V1 and Reduces the Size of Areas S1 and M1

Challenging the latter possibility, in $Dmrt5^{Tg/+}$;*Emx1-Cre* mice with excess DMRT5 in the CP (Supplementary Fig. 1C,D) neocortical area shifts were observed in hemispheres of normal size. Cortical hemisphere area size in $Dmrt5^{Tg/+}$;*Emx1-Cre* mice was 101.5 ± 3.6% of that in $Dmrt5^{Tg/Tg}$ controls ($n = 5$ litters assessed, at least 2 mice per genotype/litter). Because *Emx1, like Dmrt5*, is expressed in the CP in a high caudomedial to low rostrolateral gradient, *Dmrt5* was overexpressed in $Dmrt5^{Tg/+}$;*Emx1-Cre* mice following its normal gradient. Heterozygous, $Dmrt5^{Tg/+}$;*Emx1-Cre* animals were examined because homozygous mice ($Dmrt5^{Tg/Tg}$; *Emx1-Cre*) showed early lethality, perhaps caused by persistent expression of *Dmrt5* in post-mitotic cortical cells (Supplementary Fig. 1E).

In whole-mount brains processed for ISH at P7, the expression patterns of *Cdh6, Cdh8, Rorβ*, and *Lmo4*, which demarcate neocortical areas, were examined. The results revealed a larger V1 in $Dmrt5^{Tg/+}$;*Emx1-Cre* mice than in $Dmrt5^{Tg/Tg}$ controls (Fig. 4A and data not shown). Changes in the surface areas of V1, S1, and M1 were quantified as previously (Fig. 4B). The ratio of V1 to total hemisphere size was significantly expanded in $Dmrt5^{Tg/+}$;*Emx1-Cre* mice compared with $Dmrt5^{Tg/Tg}$ controls, appearing roughly 50% larger. Consistent with a shift in the entire area map (Fukuchi-Shimogori and Grove 2001; Hamasaki et al. 2004), the boundaries of more rostral areas, S1 and M1, moved further rostral, and both areas were significantly reduced in size. Thus, excess DMRT5 shifted the position and size of major primary sensory and motor areas in a coordinated manner along the rostrocaudal axis, as schematized in Figure 4C. Notably, the reduction of M1 and S1 undercuts a simple model that DMRT5 regulates patterning by promoting tissue growth, given that the entire CP in $Dmrt5^{Tg/+}$;*Emx1-Cre* mice is exposed to excess DMRT5, including the sites of presumptive S1 and M1. Thus, *Dmrt5* overexpression driven by *Emx1-Cre* regulates the size and position of areas along the rostrocaudal axis of the neocortex. Considering area V1 because of the clarity of its borders, comparisons among mice conditionally lacking *Dmrt5*, control mice, and $Dmrt5^{Tg/+}$;*Emx1-Cre* mice demonstrate that as the level of DMRT5 increases, V1 is progressively larger. These findings support the hypothesis that the level at which *Dmrt5* is expressed differentially regulates the neocortical area map.

Dmrt5Tg Mice Show No Abnormalities in Cortical Signaling Centers

Diminished levels of FGF8 at the RTPC generate a smaller frontal cortex and larger caudal areas (Fukuchi-Shimogori and Grove 2001). Shifts in the area map seen with increased DMRT5, however, were not associated with changes in either the extent or levels of gene expression of the two major cortical signaling centers. Expression of *Wnt* signaling components and *Bmp4* at the cortical hem was indistinguishable among $Dmrt5^{Tg/+}$;*Emx1-Cre*, and $Dmrt5^{Tg/Tg}$;*Emx1-Cre* mice, assessed by ISH and RT-qPCR (Supplementary Fig. 4A and data not shown). Introducing excess *Dmrt5* at E10.5 with in utero microelectroporation (IUME) also failed to induce extra *Wnt3a* or *Wnt2b* expression in the hem or elsewhere (Supplementary Fig. 4B). FGF8's strong downregulation of *Dmrt5* expression (Caronia-Brown et al. 2014), and the prevalence of feedback loops between other cortical transcription factors and organizer-derived signals, suggests a potential for DMRT5 to regulate *Fgf8* expression. As in the constitutive *Dmrt5* null mouse (Saulnier et al. 2013), however, *Fgf8* and *Fgf17* expression in E12.5 *Dmrt5Tg* embryos were indistinguishable from controls (Supplementary Fig. 4C). Electroporating excess *Dmrt5* into the CP at E10.5 did not alter expression of *Fgf8* or *Fgf17* after 2 days (Supplementary Fig. 4D), or that of *Fgfr2, Fgfr3, Sprouty2*, and the *Ets* gene *Etv5*, all genes responsive to FGF8 (data not shown).

Emx2, Lhx2, and *Pax6* Expression is Altered in *Dmrt5* cKO and *Dmrt5Tg* Mice

Transcription factor genes previously implicated in cortical patterning include *Lhx2, Emx2*, and *Pax6*. In constitutively *Dmrt5* null mice, *Lhx2* and *Emx2* expression is downregulated, and

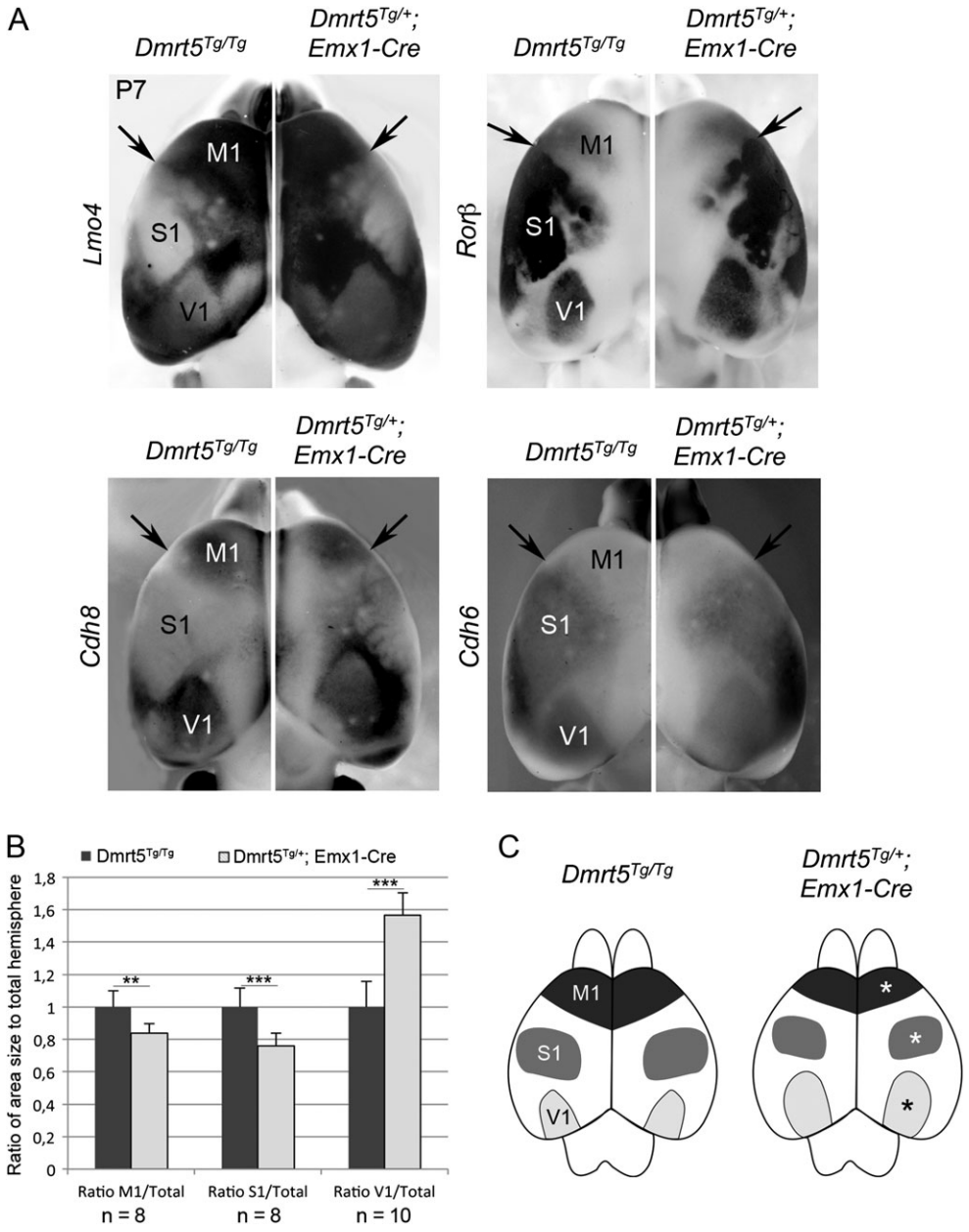

Figure 4. Excess DMRT5 changes area size and position in neocortex. (*A*) Dorsal views of P7 whole-mount brains processed with ISH for genes indicated. Control hemispheres to the left in each pair; heterozygous *Dmrt5Tg* hemispheres to the right. Hemispheres expressing excess *Dmrt5* maintain normal overall size but V1 is enlarged. (*B*) Histograms show that as a ratio of surface area to total hemisphere size, S1, and M1 are significantly reduced (**$P < 0.01$, ***$P < 0.001$). *n* = number of samples examined. (*C*) Schematic representation of the changes in primary M, S, and V area size observed in the neocortex of *Dmrt5* heterozygous *Dmrt5Tg* mice. Asterisks mark those areas that change in the *Dmrt5Tg* mouse.

expression of *Pax6* is upregulated (Saulnier et al. 2013). Expression of all three genes was assessed with ISH and RT-qPCR in the mutant mice generated for the present study. *Emx2* expression was downregulated in *Nestin-Cre* cKO and *Emx1-Cre* mice, but less so than in *Dmrt5* null mice (Saulnier et al. 2013); moreover, downregulation was only detectable at E14.5. *Lhx2* expression was clearly decreased in *Nestin-Cre* and *Emx1-Cre* cKOs, whereas *Pax6* expression increased (Fig. 5A). As would be expected, opposite changes occurred in *Dmrt5Tg mice*. Similar to the findings above, the change in *Emx2* expression, in this case an increase, only reached significance at E14.5 (Fig. 5B).

The consequence of *Dmrt5* overexpression was also evaluated by IUME into the lateral neuroepithelium of wild-type CD-1 mice at E10.5. Two days after IUME, ectopic *Dmrt5* had increased expression of *Emx2 and Lhx2*, and decreased *Pax6* expression (Fig. 5C). Thus, gain and loss of *Dmrt5* induce opposite changes in the expression of *Emx2*, *Lhx2*, and *Pax6*, independent of the status of the hem.

In *Wnt3a-Cre* cKO mice, a change in *Pax6* gene expression in the cortical hem was striking, although consistent with findings described above. In wild-type mice, the hem expresses *Dmrt5*, but specifically excludes expression of *Pax6*, which

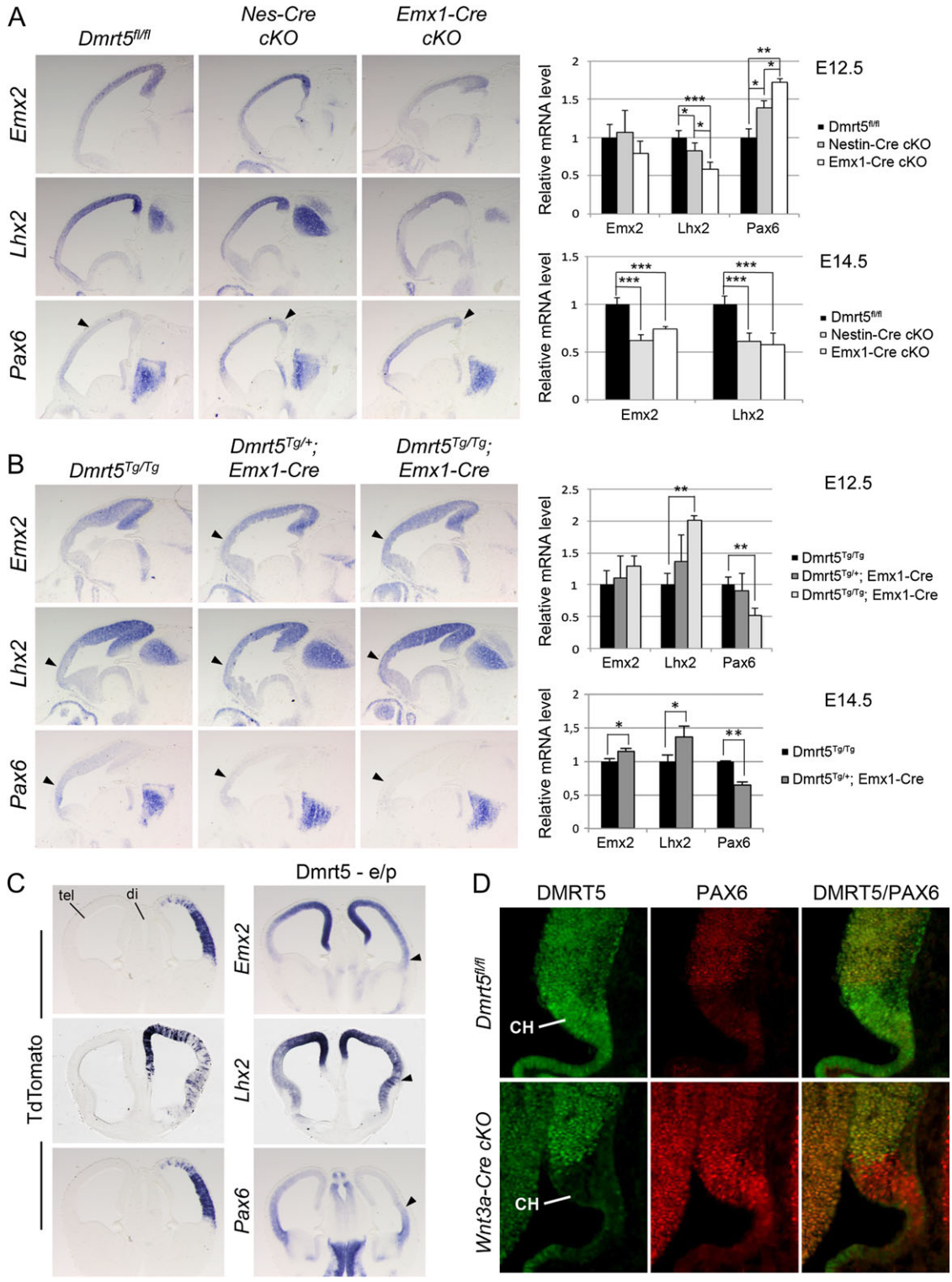

Figure 5. Altered levels of *Dmrt5* change expression of genes implicated in area map formation. (*A* and *B*) Sagittal sections through E12.5 brains processed with ISH for indicated genes, and plots of gene expression changes measured in the dorsal telencephalon by RT-qPCR. (*A*) In *Nestin-Cre* and *Emx1-Cre* cKO mice, *Lhx2* expression is downregulated and *Pax6* upregulated (compare *Pax6* expression in the caudal part of the cortex indicated by arrowheads). Measured by RT-qPCR, *Emx2* is not significantly reduced until E14.5. (*B*) Excess DMRT5 upregulates expression of *Lhx2* and downregulates *Pax6* (compare expression levels at arrowheads). As in cKO mice, the change in *Emx2* expression as assessed by RT-qPCR reaches significance at E14.5 (*$P < 0.05$, **$P < 0.01$, ***$P < 0.001$). (*C*) Overexpression of *Dmrt5* with IUME at E10.5, upregulated *Emx2* and *Lhx2* expression at E12.5, and downregulated *Pax6* (arrowheads). The sites of *Dmrt5* electroporation are marked by ISH for coelectroporated tdTomato. (*D*) High magnification views of the hem in E12.5 control and *Wnt3a-Cre* cKO embryos in coronal sections processed with IFl for DMRT5 and PAX6. In control embryos, the cortical hem shows DMRT5, but not PAX6 IFl; *Wnt3a-Cre* cKO embryos exhibit ectopic PAX6 IFl in the hem. CH, cortical hem.

extends through neighboring CP. When *Dmrt5* is selectively removed from the hem, the *Pax6* gradient in the CP was unaffected, as expected, but now the hem strongly expressed *Pax6* (Fig. 5*D*).

Opposite effects on expression of *Emx2* and *Pax6* by a given manipulation of DMRT5 were predictable, given negative regulation between PAX6 and EMX2 themselves (Muzio et al. 2002). Yet, upregulation of *Pax6* expression in the cortex of *Emx1-Cre* cKO, *Nestin-Cre* cKO, and *Dmrt5* null mice was puzzling given that *Lhx2* is required for *Pax6* expression (Shetty et al. 2013), and yet is downregulated in these mutants. These observations highlight the complexity of the transcriptional regulation of the *Pax6* locus and the importance of DMRT5 in this process.

Loss of *Dmrt3* Results in Reduction of Caudomedial Neocortical Areas

Like *Dmrt5*, the related gene *Dmrt3* is expressed in cortical progenitors in a high caudomedial to low rostrolateral gradient (Konno et al. 2012) suggesting that *Dmrt3* may also contribute to cortical patterning. To test this possibility, we generated *Dmrt3* constitutive null mice. Cerebral hemispheres and the hippocampus of *Dmrt3* mutants were decreased in size compared with control mice (hemisphere reduction: 17.7 ± 7.2%, $n = 7$), the reduction observed being less severe than in *Dmrt5* null mice (Fig. 6 and Supplementary Fig. 5). At the cortical hem, expression of *Wnt* and *Bmp* genes and WNT signaling activity was reduced but much less severely than in *Dmrt5* null mice (Fig. 6*A*). Expression of *Emx2* was downregulated, again much less drastically than in *Dmrt5* null mice. *Pax6* was upregulated and its expression spread medially in the cortex of $Dmrt3^{-/-}$ embryos, but again less strongly than in $Dmrt5^{-/-}$ embryos. *Pax6* was conversely downregulated upon *Dmrt3* overexpression by in utero electroporation, as observed with *Dmrt5* (Fig. 6*A*,*B*). Thus, *Dmrt3* causes a similar, albeit milder, phenotype to that of *Dmrt5* when constitutively deleted or overexpressed.

Dmrt3 null mice survive birth, so that distinct neocortical areas could be examined postnatally with the gene expression markers used above. In P7 whole-mount brains and sagittal sections processed for ISH, V1 appeared smaller in size (Fig. 6*C* and Supplementary Fig. 5). Based on the dorsal view of the whole-mount images, the ratio of V1 areas to total hemisphere size was estimated to be about 22% reduced (Fig. 6*D*,*E*). These observations are consistent with a role for *Dmrt3* in regulating the neocortical area map. As for *Dmrt5*, this hypothesis will require future testing in a mouse line with gain of *Dmrt3* function.

Dmrt5 Expression is Negatively Regulated by DMRT5 and DMRT3

Given the coexpression of *Dmrt3* and *Dmrt5* in the same progenitor cells and in matching expression gradients (Konno et al. 2012), combined with both the similarities and differences in the patterning defects in *Dmrt3* and *Dmrt5* null mice, we asked whether DMRT3 and DMRT5 interact to regulate their gene expression. We assessed *Dmrt5* expression levels in *Dmrt3* constitutive null embryos and *Dmrt3* expression levels in *Dmrt5* mutants with ISH and RT-qPCR. The level of *Dmrt3* was reduced in *Dmrt5* null KO mice and that of *Dmrt5* increased in *Dmrt3* null KO mice (Fig. 7 and data not shown), demonstrating that DMRT5 upregulates *Dmrt3* expression, whereas DMRT3 downregulates expression of *Dmrt5*. A third member of the *Dmrt* gene family, *Dmrt4* (*Dmrta1*), is expressed in an opposite gradient to *Dmrt3/5* and is positively regulated by PAX6 (Kikkawa et al. 2013). Given the opposing gene expression patterns, upregulation of *Dmrt4* expression in *Dmrt3* and *Dmrt5* null mutant mice was as predicted (Fig. 7 and data not shown).

Expression of *Dmrt5* is not only downregulated by DMRT3 but also by DMRT5 itself. In E12.5 $Dmrt5^{Tg/Tg}$; *Emx1-Cre* mice, a higher level of total DMRT5 protein, compared with control mice, was as expected evident with DMRT5-IFl, and western blotting. In heterozygous $Dmrt5^{Tg/+}$; *Emx1-Cre* mice, the level of DMRT5 detected appeared intermediate between levels in homozygous $Dmrt5^{Tg/Tg}$; *Emx1-Cre* mice and controls. In western blots, DMRT5 levels were estimated in heterozygous and homozygous *Dmrt5Tg* mice, respectively, as 1.8- and 2.6-fold times the level in controls (Fig. 8*A*,*B*). Surprisingly, ISH and RT-qPCR assays revealed that while the level of transgenic *Dmrt5* transcript, reflected by *Dmrt5*-IRES-linked *eGFP* expression, was increased in the cortex of heterozygous and homozygous *Dmrt5Tg* mice, the level of endogenous *Dmrt5* transcript was diminished (Fig. 8*C*).

Conversely, the level of *Dmrt5* exon 2 deleted transcripts was increased in the cortical epithelium of *Emx1-Cre* cKO mice (Fig. 8*D*). These findings suggest that *Dmrt5* mRNA level is tightly controlled in a negative feedback loop by DMRT5 itself and DMRT3 (Fig. 8*E*). Because abnormal levels of *Dmrt* genes cause marked aberrations in cortical patterning, including the neocortical area map, such fine control of their expression is consistent with a critical role in normal cortical development.

Discussion

Dmrt5 is Directly Required for Several Processes in Cortical Patterning

Constitutive loss of *Dmrt5* causes the hippocampus and caudomedial neocortex to shrink, and the boundary of paleocortex to shift dorsally, strongly resembling cortical changes in hem-ablated mice (Konno et al. 2012; Saulnier et al. 2013; Caronia-Brown et al. 2014). Given that constitutive deletion of *Dmrt5* virtually obliterates the hem, a ready conclusion is that *Dmrt5* has its effects on cortex because of the loss of hem WNT and BMP signals. In the present study, however, *Dmrt5* was conditionally deleted from cortical progenitors after the hem had formed. No overt defects were seen in the hem with respect to its size, morphology, or expression of a variety of genes associated with WNT or BMP signaling. Nonetheless, abnormalities in the hippocampus and neocortex, and at the boundary between neocortex and paleocortex, were similar to those observed in constitutive *Dmrt5* null mice. These findings indicate that *Dmrt5* has several important functions in forebrain development, first establishing the hem, second acting in cortical progenitor cells to direct functional cortical subdivisions, and third contributing to the correct formation of the neocortical area map.

A parsimonious interpretation is that DMRT5 loss in the CP and consequent influences on *Dmrt* downstream effector genes are also responsible for the cortical defects in the constitutively *Dmrt5* null mouse. The defects are more severe in the null than in cKO mice because *Dmrt5* was deleted earlier in development. This interpretation is supported by the greater severity of cortical defects in *Emx1-Cre* cKO mice than in *Nestin-Cre* cKO animals, given that *Emx1-Cre* drives gene deletion in the CP about a day

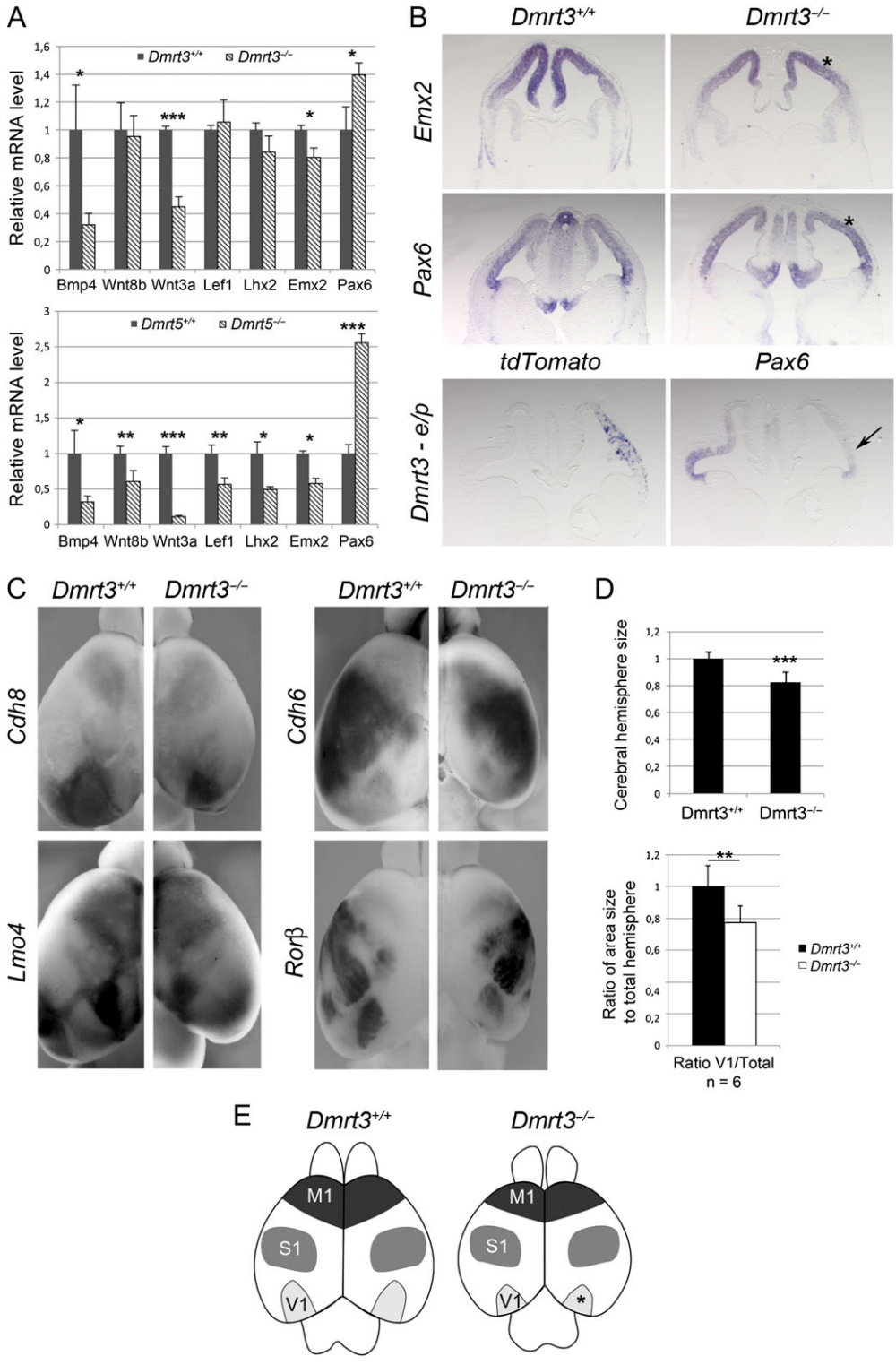

Figure 6. V1 reduced in *Dmrt3*$^{-/-}$ mice with modest reduction of cortical size and hem gene expression. (*A*) RT-qPCR analysis of the expression of the indicated genes in the cortex of *Dmrt3*$^{-/-}$ mice and, for comparison, in *Dmrt5*$^{-/-}$ mice (*$P < 0.05$, **$P < 0.01$, ***$P < 0.001$). (*B*) Coronal brain sections of E12.5 embryos. Expression of *Emx2* is decreased in *Dmrt3*$^{-/-}$ embryos (asterisk) and *Pax6* is increased (see asterisks). IUME of *Dmrt3* downregulates *Pax6* expression (arrow). (*C*) Dorsal views of P7 whole-mount brains processed by ISH for the indicated genes. (*D*) Graphs representing the overall change in hemisphere size in *Dmrt3* null mice, and the disproportionate reduction of V1 (**$P < 0.01$, ***$P < 0.001$). (*E*) Schematic representation of the changes in primary M, S, and V area size observed in the neocortex of the *Dmrt3* cKO mice.

before *Nestin-Cre* (Gorski et al. 2002; Sahara and O'Leary 2009; Shetty et al. 2013). Thus, alteration in the position of the neocortical/paleocortical boundary was observed in *Emx1-Cre* but not in *Nestin-Cre* cKO mice, suggesting that DMRT5, like LHX2 (Chou et al. 2009) regulates this boundary before E11.5 and the start of substantial cortical neurogenesis. Additionally, a reduced hippocampus was observed in both cKO mice, but the reduction was more severe in *Emx1-Cre* than in *Nestin-Cre* cKO mice.

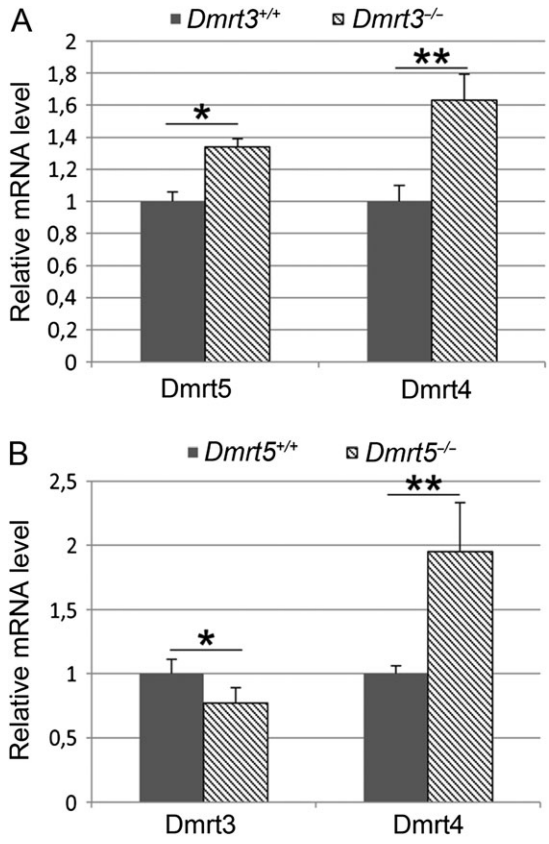

Figure 7. Interactions between *Dmrt* genes. (A) RT-qPCR of the expression of *Dmrt5* and *Dmrt4* in the cortex of WT and *Dmrt3*$^{-/-}$ embryos. Both genes are upregulated in *Dmrt3*$^{-/-}$ E12.5 embryos. (*B*) Expression of *Dmrt3* and *Dmrt4* in the cortex of WT and *Dmrt5*$^{-/-}$ embryos. *Dmrt4* is upregulated in *Dmrt5*$^{-/-}$ embryos; *Dmrt3* is decreased (*$P < 0.05$, **$P < 0.01$, ***$P < 0.001$).

DMRT5 Controls the Size and Position of Neocortical Areas

Both the constitutive null *Dmrt5* mutant (Saulnier et al. 2013) and cKO *Dmrt5* mutants have smaller cortical hemispheres than wild-type mice, indicating an important function for *Dmrt5* in growth control, which remains to be fully characterized. Because *Dmrt5* expression is higher caudomedially, loss of *Dmrt5* might cause the notably disproportionate reduction in the growth of caudomedial cortex. We therefore determined the boundaries of cortical regions and the size and position of neocortical areas in mice conditionally overproducing DMRT5 (*Dmrt5Tg* mice), which had normally sized cortical hemispheres. In *Dmrt5Tg* mice, excess DMRT5 protein was generated throughout the CP, but did not enlarge the hippocampus, or the overall surface area of the neocortex. In this context, V1 was roughly half larger in heterozygous *Dmrt5Tg* mice than in control mice, and M1 and S1 were smaller. That is, DMRT5 regulated the size and position of areas in a manner corresponding to the caudomedial high to rostrolateral low expression gradient of *Dmrt5*, retained in the *Dmrt5*$^{Tg/+}$; *Emx1-Cre* mice. These findings are hard to square with the hypothesis that DMRT5's effects on tissue growth caused the neocortical area changes, given that DMRT5 was also available in excess at the sites of M1 and S1 generation, yet these areas were reduced. Also inconsistent with a model in which DMRT5 regulates regional boundaries in cortex by promoting region-specific tissue growth is the observation that ventrolateral cortex, where *Dmrt5* expression is lowest, enlarges with deletion of *Dmrt5*.

Interactions Between DMRT5 and Other Known Cortical Transcription Factors

DMRT5 regulates the expression of several transcription factors whose roles in patterning the cerebral cortex have been more thoroughly explored. They include EMX2 (Hamasaki et al. 2004; Zembrzycki et al. 2015), PAX6 (Bishop 2000; Bishop et al. 2002; Backman et al. 2005; Zembrzycki et al. 2013), and LHX2 (Mangale et al. 2008; Chou et al. 2009; Shetty et al. 2013). Findings from the present study suggest that DMRT5 both interacts with these transcription factors in cortical patterning and functions independently.

Similar to excess DMRT5, excess EMX2 generates a neocortex with an abnormally large V1 and correspondingly smaller S1 and M1 (Hamasaki et al. 2004); thus, the relationship between *Emx2* and *Dmrt5* is particularly relevant. *Dmrt5* expression is unaffected in mice lacking *Emx2*, whereas *Emx2* expression is downregulated in *Dmrt5* null mice, indicating that *Emx2* lies downstream of *Dmrt5* (Saulnier et al. 2013). The most dramatic effects of manipulating DMRT5 levels on the neocortical area map, however, seem likely to reflect an activity of DMRT5 independent of EMX2. Excess DMRT5 in the CP from E10.5 caused extensive changes in the neocortical area map, but only a modest and relatively late (E14.5) upregulation of *Emx2* expression. We suggest that in wild-type mice DMRT5 acts directly on the neocortex but in concert with EMX2. Such a cooperation would explain a previous finding, namely that decreasing the excess FGF8 observed in *Emx2* null mice rescues at least part of the *Emx2* mutant cortical phenotype (Fukuchi-Shimogori and Grove 2003). Excess FGF8 would also downregulate *Dmrt5* expression, so that reducing the FGF8 surplus would mitigate a joint *Emx2*/*Dmrt5* phenotype.

Excess DMRT5 reduces expression of *Pax6*, which could also contribute to the neocortical phenotype observed in *Dmrt5*$^{Tg/+}$; *Emx1-Cre* mice. Reduced rostral and expanded caudal areas have been reported in mice constitutively lacking *Pax6* but because these mice die at birth, neocortical areas could not be definitively identified with postnatal gene expression patterns (Bishop 2000; Bishop et al. 2002). Conditional deletion of *Pax6* in cortical progenitors, utilizing the same *Emx1-IRES-Cre* used in the present study (Gorski et al. 2002), halves the size of the cortical hemispheres and hugely diminishes the absolute size of S1 with no overt disproportional changes in the size of either V1 or frontal cortex (Zembrzycki et al. 2013). Reducing *Pax6* expression in *Dmrt5*$^{Tg/+}$;*Emx1-Cre* mice might therefore contribute to a smaller S1, but not to the greatly enlarged V1. That *Dmrt5*$^{Tg/+}$;*Emx1-Cre* cortical hemispheres were indistinguishable in size from wild-type mice is further generally inconsistent with a role for *Pax6* reduction in the *Dmrt5*$^{Tg/+}$;*Emx1-Cre* phenotype.

DMRT5 upregulates expression of *Lhx2*, and in *Emx1-Cre Dmrt5* cKO mice *Lhx2* expression is reduced by about half (Fig. 7A,C). With conditional deletion of *Lhx2* at E10.5, utilizing the same *Emx1-Cre* driver line as in the present study (Gorski et al. 2002), neocortical progenitors are re-fated to generate neurons for paleocortex (Chou et al. 2009). Heterozygous *Lhx2* cKO mutants, however, do not show this phenotype (Chou et al. 2009). In the *Emx1-Cre Dmrt5* cKO mice, a shift in the boundary between neocortex and paleocortex is observed, much more modest than in the *Emx1-Cre Lhx2* cKOs. Thus, halving the levels of *Lhx2* could potentially contribute to this defect. *Gli3* is another transcription factor involved in regulating the separation between the neocortex and paleocortex

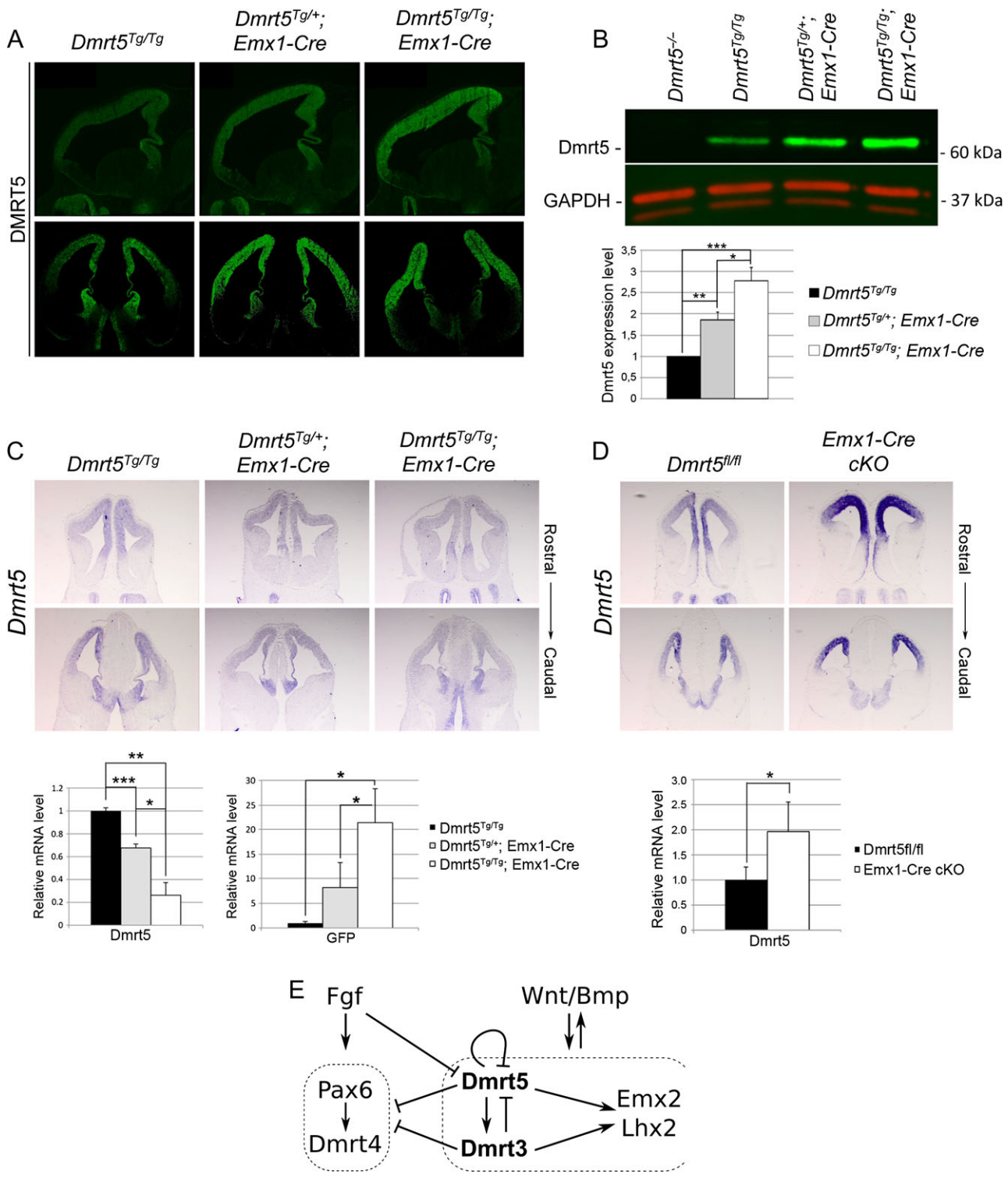

Figure 8. Negative autoregulation by *Dmrt5*. (*A*) Sagittal (top) and coronal (bottom) brain sections processed by IFl for DMRT5 on E12.5 control (*Dmrt5*$^{Tg/Tg}$), *Dmrt5*$^{Tg/+}$; *Emx1-Cre*, and *Dmrt5*$^{Tg/Tg}$;*Emx1-Cre* embryos. DMRT5-IFl is increased and more uniform in *Dmrt5Tg* embryos. (*B*) Western blot shows a higher level of DMRT5 protein in the dorsal telencephalon of E12.5 *Dmrt5*$^{Tg/+}$;*Emx1-Cre* and *Dmrt5*$^{Tg/Tg}$;*Emx1-Cre* mice than in control non-Cre-excised *Dmrt5*$^{Tg/Tg}$ mice. *Dmrt5*$^{-/-}$ embryos were used as negative controls. Bar graph shows quantification of three distinct western blots. For each sample, the intensity of the Dmrt5 band was divided by the intensity of the GAPDH band to account for loading differences. Expression levels in the *Dmrt5*$^{Tg/+}$;*Emx1-Cre* and *Dmrt5*$^{Tg/Tg}$;*Emx1*-Cre embryos were calculated relative to the controls (*Dmrt5*$^{Tg/Tg}$), which was assigned a value of 1 (*$P < 0.05$, **$P < 0.01$, ***$P < 0.001$). (*C* and *D*) ISH for *Dmrt5*, E12.5 coronal brain sections (top); quantitative RT-qPCR analysis of *Dmrt5* (bottom) in the dorsal telencephalon of E12.5 embryos. Endogenous *Dmrt5* transcripts are reduced in *Dmrt5*$^{Tg/+}$;*Emx1-Cre* and *Dmrt5*$^{Tg/Tg}$;*Emx1-Cre* embryos and upregulated in *Emx1-Cre* cKO (*$P < 0.05$, **$P < 0.01$, ***$P < 0.001$). *Dmrt5*$^{Tg/Tg}$ or *Dmrt5*$^{fl/fl}$ were used as controls. Transgenic *Dmrt5* expression in *Dmrt5*$^{Tg/+}$;*Emx1-Cre* and *Dmrt5*$^{Tg/Tg}$;*Emx1-Cre* embryos was evaluated using *GFP* primers. (*E*) Model of *Dmrt5* and *Dmrt3* gene action in the CP downstream of cortical hem signals based on results from this work and others (Konno et al. 2012; Saulnier et al. 2013).

(Amaniti et al. 2015). Its expression is largely unaffected in *Dmrt5*$^{-/-}$ and *Dmrt3*$^{-/-}$ mutants (Saulnier et al. 2013).

Our results allow us to consider only limited potential transcription factor interactions. Functional interactions among DMRT5, EMX2, PAX6, and LHX2 with respect to cortical subdivision and formation of the neocortical area map require further investigation. Direct transcriptional regulation between members of this group, as well as overlap in their transcriptional targets, also remain to be determined. Genes that control patterning of cerebral cortex and the formation of the neocortical area map are also tightly involved in the control of the proliferation/differentiation of cortical progenitors. Several studies have associated *Dmrt* with proneural genes (Huang et al. 2005; Yoshizawa et al. 2011). Further functions of the DMRT subgroup in regulating proneural genes, and in neurogenesis more generally, remains to be explored.

DMRT3 also Contributes to the Control of Cortical Development

Dmrt genes have been studied extensively for their roles in sex determination and sexual differentiation, conserved widely across metazoans (Hong et al. 2007; Bellefroid et al. 2013). Recently, *Dmrt* genes have been found to have functions in neural development, including neuronal specification in the vertebrate spinal cord (Andersson et al. 2012). *Dmrt3, Dmrt4*, and *Dmrt5* belong to a *Dmrt* gene subfamily that contains a DMA domain. All three are expressed in gradients in the CP, and their functions and interactions in cortical development have yet to be fully investigated. Our analysis of the phenotype of *Dmrt3* constitutively null mice suggests that *Dmrt3* has a similar function to *Dmrt5* in cortical development, including a role in generating the neocortical area map. The importance of *Dmrt3* in cortical development inferred from the phenotype of *Dmrt3* null KO mice is likely to be underevaluated given the fact that the absence of *Dmrt3* may be compensated by the increase of *Dmrt5*.

How *Dmrt3* functions with *Dmrt5* to control cortical patterning is unclear. *Dmrt3* mRNA is reduced in *Dmrt5* constitutive null mice suggesting that *Dmrt3* may function downstream of *Dmrt5*. Whether they act in concert and whether they directly or indirectly regulate *Wnt, Bmp, Emx2, Lhx2*, or *Pax6* gene expression remain to be addressed. Finally, the possible role of *Dmrt4* in cortical patterning remains to be considered.

Negative Autoregulation of Dmrt5

Negative feedback is an important component of many biological networks. Computational and experimental approaches have shown that genes regulated by negative feedback have more stable expression than other genes (Hasty et al. 2002). Our identification of negative feedback in *Dmrt5* regulation in the developing telencephalon highlights the probable importance of maintaining appropriate levels of its expression in the fast growing telencephalic vesicles during embryonic development.

Our evidence for negative autoregulation comes from the finding that endogenous *Dmrt5* mRNA levels are reduced in *Dmrt5Tg* mice and that *Dmrt5* exon 2 deleted transcript levels are increased in *Emx1-Cre Dmrt5* cKO mice. Despite the reduction of endogenous *Dmrt5* mRNA level in *Dmrt5*-overexpressing *Dmrt5Tg* mice, total DMRT5 protein levels were elevated, presumably because of the highly efficient transcription of the *Dmrt5* transgene at the ROSA26 locus. We cannot exclude that other mechanisms such as posttranscriptional ones may also participate in the elevation of DMRT5 protein levels observed in the *Dmrt5Tg* mice. In transgenic mice overexpressing the human PAX6 gene, elevated PAX6 protein levels are observed despite negative feedback autoregulation of *Pax6* expression (Manuel et al. 2007).

The negative transcriptional autoregulation of *Dmrt5* may be direct, as in the case of *Pax6* autoregulation (Aota et al. 2003; Kleinjan et al. 2004), or indirect given that DMRT5 influences the expression of many other transcription factors (Fig. 5). Autoregulation has been demonstrated, however, for another member of the *Dmrt* gene family, *Dmrt1*, which is critical for testis development (Murphy et al. 2010). Negative regulation of *Dmrt5* further involves DMRT3, given that *Dmrt5* mRNA is increased in the *Dmrt3* null KO. While the mechanisms controlling *Dmrt5* expression are likely to be complex and remain to be investigated, our findings implicate negative autoregulation as an important stabilizing component of DMRT5 protein level in the developing cortical neuroepithelium.

Supplementary Material

Supplementary material is available at *Cerebral Cortex* online.

Funding

This work was supported by grants from the FNRS (FRFC 6973823), the Walloon Region (First International project "CORTEX), the Wiener-Anspach Foundation, and the Fonds pour la Recherche Médicale dans le Hainaut (FMRH), Hoguet, J. Brachet et David et Alice Van Buuren to E.B. Work in the laboratories of E.A.G. and D.Z. was supported by NIH grants MH103211 and GM15952, respectively. S.D.C. was a FNRS postdoctoral fellow, M.K. a First International postodoctoral fellow, J.P. a FNRS doctoral fellow, and C.K.M. a NSF predoctoral fellow. E.D. is supported by a Wallonie-Bruxelles International (WBI) doctoral fellowship.

Notes

The authors acknowledge S. Garel, P. Vanderhaeghen for providing the Wnt3a-IRES-Cre (this line was generated by M. Yoshida in the laboratory of E. Grove), Emx1-IRES-Cre, and Nestin-IRES-Cre mouse lines, M. Li for providing the DMRT5 antibody, and S. Tole for providing plasmids. We are grateful to S. Kricha for technical assistance and L. Delhaye for animal care and genotyping. Fluorescence microscopy images were taken at the Center for Microscopy and Molecular Imaging (CMMI), which is supported by the Hainaut-Biomed FEDER program. *Conflict of Interest*: None declared.

References

Agarwala S, Sanders TA, Ragsdale CW. 2001. Sonic hedgehog control of size and shape in midbrain pattern formation. Science. 291:2147–2150.

Amaniti EM, Fu C, Lewis S, Saisana M, Magnani D, Mason JO, Theil T. 2015. Expansion of the piriform cortex contributes to corticothalamic pathfinding defects in Gli3 conditional mutants. Cereb Cortex. 25:460–471.

Andersson LS, Larhammar M, Memic F, Wootz H, Schwochow D, Rubin CJ, Patra K, Arnason T, Wellbring L, Hjalm G, et al. 2012. Mutations in DMRT3 affect locomotion in horses and spinal circuit function in mice. Nature. 488:642–646.

Aota S, Nakajima N, Sakamoto R, Watanabe S, Ibaraki N, Okazaki K. 2003. Pax6 autoregulation mediated by direct interaction of Pax6 protein with the head surface ectoderm-specific enhancer of the mouse Pax6 gene. Dev Biol. 257:1–13.

Asami M, Pilz GA, Ninkovic J, Godinho L, Schroeder T, Huttner WB, Gotz M. 2011. The role of Pax6 in regulating the orientation and mode of cell division of progenitors in the mouse cerebral cortex. Development. 138:5067–5078.

Assimacopoulos S, Kao T, Issa NP, Grove EA. 2012. Fibroblast growth factor 8 organizes the neocortical area map and regulates sensory map topography. J Neurosci. 32:7191–7201.

Bachler M, Neubuser A. 2001. Expression of members of the Fgf family and their receptors during midfacial development. Mech Dev. 100:313–316.

Backman M, Machon O, Mygland L, van den Bout CJ, Zhong W, Taketo MM, Krauss S. 2005. Effects of canonical Wnt signaling on dorso-ventral specification of the mouse telencephalon. Dev Biol. 279:155–168.

Bellefroid EJ, Leclere L, Saulnier A, Keruzore M, Sirakov M, Vervoort M, De Clercq S. 2013. Expanding roles for the evolutionarily conserved Dmrt sex transcriptional regulators during embryogenesis. Cell Mol Life Sci. 70:3829–3845.

Bishop KM. 2000. Regulation of area identity in the mammalian neocortex by Emx2 and Pax6. Science. 288:344–349.

Bishop KM, Rubenstein JL, O'Leary DD. 2002. Distinct actions of Emx1, Emx2, and Pax6 in regulating the specification of areas in the developing neocortex. J Neurosci. 22:7627–7638.

Bulchand S, Grove EA, Porter FD, Tole S. 2001. LIM-homeodomain gene Lhx2 regulates the formation of the cortical hem. Mech Dev. 100:165–175.

Caronia-Brown G, Yoshida M, Gulden F, Assimacopoulos S, Grove EA. 2014. The cortical hem regulates the size and patterning of neocortex. Development. 141:2855–2865.

Chen H, Chedotal A, He Z, Goodman CS, Tessier-Lavigne M. 1997. Neuropilin-2, a novel member of the neuropilin family, is a high affinity receptor for the semaphorins Sema E and Sema IV but not Sema III. Neuron. 19:547–559.

Cholfin JA, Rubenstein JL. 2007. Patterning of frontal cortex subdivisions by Fgf17. Proc Natl Acad Sci USA. 104:7652–7657.

Cholfin JA, Rubenstein JL. 2008. Frontal cortex subdivision patterning is coordinately regulated by Fgf8, Fgf17, and Emx2. J Comp Neurol. 509:144–155.

Chou SJ, Perez-Garcia CG, Kroll TT, O'Leary DD. 2009. Lhx2 specifies regional fate in Emx1 lineage of telencephalic progenitors generating cerebral cortex. Nat Neurosci. 12: 1381–1389.

Crossley PH, Martin GR. 1995. The mouse Fgf 8 gene encodes a family of polypeptides and is expressed in regions that direct outgrowth and patterning in the developing embryo. Development. 121:439–451.

Crossley PH, Martinez S, Ohkubo Y, Rubenstein JL. 2001. Coordinate expression of Fgf8, Otx2, Bmp4, and Shh in the rostral prosencephalon during development of the telencephalic and optic vesicles. Neuroscience. 108:183–206.

Fukuchi-Shimogori T, Grove EA. 2001. Neocortex patterning by the secreted signaling molecule FGF8. Science. 294:1071–1074.

Fukuchi-Shimogori T, Grove EA. 2003. Emx2 patterns the neocortex by regulating FGF positional signaling. Nat Neurosci. 6:825–831.

Furuta Y, Piston DW, Hogan BL. 1997. Bone morphogenetic proteins (BMPs) as regulators of dorsal forebrain development. Development. 124:2203–2212.

Gaitanis JN, Walsh CA. 2004. Genetics of disorders of cortical development. Neuroimaging Clin N Am. 14:219–229.

Garel S, Huffman KJ, Rubenstein JLR. 2003. Molecular regionalization of the neocortex is disrupted in Fgf8 hypomorphic mutants. Development. 130:1903–1914.

Genove G, Glick BS, Barth AL. 2005. Brighter reporter genes from multimerized fluorescent proteins. Biotechniques. 39:814, 816, 818 passim.

Gorski JA, Talley T, Qiu M, Puelles L, Rubenstein JL, Jones KR. 2002. Cortical excitatory neurons and glia, but not GABAergic neurons, are produced in the Emx1-expressing lineage. J Neurosci. 22:6309–6314.

Gotz M, Stoykova A, Gruss P. 1998. Pax6 controls radial glia differentiation in the cerebral cortex. Neuron. 21:1031–1044.

Grove EA, Tole S, Limon J, Yip L, Ragsdale CW. 1998. The hem of the embryonic cerebral cortex is defined by the expression of multiple Wnt genes and is compromised in Gli3-deficient mice. Development. 125:2315–2325.

Hamasaki T, Leingartner A, Ringstedt T, O'Leary DD. 2004. EMX2 regulates sizes and positioning of the primary sensory and motor areas in neocortex by direct specification of cortical progenitors. Neuron. 43:359–372.

Hasty J, McMillen D, Collins JJ. 2002. Engineered gene circuits. Nature. 420:224–230.

Hong CS, Park BY, Saint-Jeannet JP. 2007. The function of Dmrt genes in vertebrate development: it is not just about sex. Dev Biol. 310:1–9.

Hu WF, Chahrour MH, Walsh CA. 2014. The diverse genetic landscape of neurodevelopmental disorders. Annu Rev Genomics Hum Genet. 15:195–213.

Huang X, Hong CS, O'Donnell M, Saint-Jeannet JP. 2005. The doublesex-related gene, XDmrt4, is required for neurogenesis in the olfactory system. Proc Natl Acad Sci USA. 102:11349–11354.

Kikkawa T, Obayashi T, Takahashi M, Fukuzaki-Dohi U, Numayama-Tsuruta K, Osumi N. 2013. Dmrta1 regulates proneural gene expression downstream of Pax6 in the mammalian telencephalon. Genes Cells. 18:636–649.

Kleinjan DA, Seawright A, Childs AJ, van Heyningen V. 2004. Conserved elements in Pax6 intron 7 involved in (auto)regulation and alternative transcription. Dev Biol. 265:462–477.

Konno D, Iwashita M, Satoh Y, Momiyama A, Abe T, Kiyonari H, Matsuzaki F. 2012. The mammalian DM domain transcription factor Dmrta2 is required for early embryonic development of the cerebral cortex. PLoS One. 7:e46577.

Lee SM, Tole S, Grove E, McMahon AP. 2000. A local Wnt-3a signal is required for development of the mammalian hippocampus. Development. 127:457–467.

Ma L, Harada T, Harada C, Romero M, Hebert JM, McConnell SK, Parada LF. 2002. Neurotrophin-3 is required for appropriate establishment of thalamocortical connections. Neuron. 36: 623–634.

Mallamaci A, Muzio L, Chan CH, Parnavelas J, Boncinelli E. 2000. Area identity shifts in the early cerebral cortex of Emx2$^{-/-}$ mutant mice. Nat Neurosci. 3:679–686.

Mangale VS, Hirokawa KE, Satyaki PR, Gokulchandran N, Chikbire S, Subramanian L, Shetty AS, Martynoga B, Paul J, Mai MV, et al. 2008. Lhx2 selector activity specifies cortical identity and suppresses hippocampal organizer fate. Science. 319:304–309.

Manuel M, Georgala PA, Carr CB, Chanas S, Kleinjan DA, Martynoga B, Mason JO, Molinek M, Pinson J, Pratt T, et al. 2007. Controlled overexpression of Pax6 in vivo negatively autoregulates the Pax6 locus, causing cell-autonomous defects of late cortical progenitor proliferation with little effect on cortical arealization. Development. 134:545–555.

Mi D, Carr CB, Georgala PA, Huang YT, Manuel MN, Jeanes E, Niisato E, Sansom SN, Livesey FJ, Theil T, et al. 2013. Pax6 exerts regional control of cortical progenitor proliferation

via direct repression of Cdk6 and hypophosphorylation of pRb. Neuron. 78:269–284.

Monuki ES, Porter FD, Walsh CA. 2001. Patterning of the dorsal telencephalon and cerebral cortex by a roof plate-Lhx2 pathway. Neuron. 32:591–604.

Murphy MW, Sarver AL, Rice D, Hatzi K, Ye K, Melnick A, Heckert LL, Zarkower D, Bardwell VJ. 2010. Genome-wide analysis of DNA binding and transcriptional regulation by the mammalian Doublesex homolog DMRT1 in the juvenile testis. Proc Natl Acad Sci USA. 107:13360–13365.

Muzio L, Di Benedetto B, Stoykova A, Boncinelli E, Gruss P, Mallamaci A. 2002. Emx2 and Pax6 control regionalization of the pre-neuronogenic cortical primordium. Cereb Cortex. 12:129–139.

Muzio L, Soria JM, Pannese M, Piccolo S, Mallamaci A. 2005. A mutually stimulating loop involving emx2 and canonical wnt signalling specifically promotes expansion of occipital cortex and hippocampus. Cereb Cortex. 15:2021–2028.

Nauta WJH, Feirtag M. 1986. Fundamental Neuroanatomy. New York: W.H.Freeman and Company.

Nyabi O, Naessens M, Haigh K, Gembarska A, Goossens S, Maetens M, De Clercq S, Drogat B, Haenebalcke L, Bartunkova S, et al. 2009. Efficient mouse transgenesis using Gateway-compatible ROSA26 locus targeting vectors and F1 hybrid ES cells. Nucleic Acids Res. 37:e55.

Ohkubo Y, Chiang C, Rubenstein JL. 2002. Coordinate regulation and synergistic actions of BMP4, SHH and FGF8 in the rostral prosencephalon regulate morphogenesis of the telencephalic and optic vesicles. Neuroscience. 111:1–17.

Sahara S, O'Leary DD. 2009. Fgf10 regulates transition period of cortical stem cell differentiation to radial glia controlling generation of neurons and basal progenitors. Neuron. 63:48–62.

Saulnier A, Keruzore M, De Clercq S, Bar I, Moers V, Magnani D, Walcher T, Filippis C, Kricha S, Parlier D, et al. 2013. The doublesex homolog Dmrt5 is required for the development of the caudomedial cerebral cortex in mammals. Cereb Cortex. 23:2552–2567.

Shetty AS, Godbole G, Maheshwari U, Padmanabhan H, Chaudhary R, Muralidharan B, Hou PS, Monuki ES, Kuo HC, Rema V, et al. 2013. Lhx2 regulates a cortex-specific mechanism for barrel formation. Proc Natl Acad Sci USA. 110: E4913–E4921.

Sohn WJ, Ji YR, Kim HS, Gwon GJ, Chae YM, An CH, Park HD, Jung HS, Ryoo ZY, Lee S, et al. 2012. Rgs19 regulates mouse palatal fusion by modulating cell proliferation and apoptosis in the MEE. Mech Dev. 129:244–254.

Storm EE, Garel S, Borello U, Hebert JM, Martinez S, McConnell SK, Martin GR, Rubenstein JL. 2006. Dose-dependent functions of Fgf8 in regulating telencephalic patterning centers. Development. 133:1831–1844.

Tole S, Goudreau G, Assimacopoulos S, Grove EA. 2000. Emx2 is required for growth of the hippocampus but not for hippocampal field specification. J Neurosci. 20:2618–2625.

Toyoda R, Assimacopoulos S, Wilcoxon J, Taylor A, Feldman P, Suzuki-Hirano A, Shimogori T, Grove EA. 2010. FGF8 acts as a classic diffusible morphogen to pattern the neocortex. Development. 137:3439–3448.

Tronche F, Kellendonk C, Kretz O, Gass P, Anlag K, Orban PC, Bock R, Klein R, Schutz G. 1999. Disruption of the glucocorticoid receptor gene in the nervous system results in reduced anxiety. Nat Genet. 23:99–103.

Urquhart JE, Beaman G, Byers H, Roberts NA, Chervinsky E, Sullivan JO, Pilz D, Fry A, Williams SG, Bhaskar SS, et al. 2016. DMRTA2 (DMRT5) is mutated in a novel cortical brain malformation. Clin Genet. 89:724–727.

Yoshida M, Assimacopoulos S, Jones KR, Grove EA. 2006. Massive loss of Cajal-Retzius cells does not disrupt neocortical layer order. Development. 133:537–545.

Yoshida M, Suda Y, Matsuo I, Miyamoto N, Takeda N, Kuratani S, Aizawa S. 1997. *Emx1* and *Emx2* functions in development of dorsal telencephalon. Development. 124:101–111.

Yoshizawa A, Nakahara Y, Izawa T, Ishitani T, Tsutsumi M, Kuroiwa A, Itoh M, Kikuchi Y. 2011. Zebrafish Dmrta2 regulates neurogenesis in the telencephalon. Genes Cells. 16: 1097–1109.

Zembrzycki A, Chou SJ, Ashery-Padan R, Stoykova A, O'Leary DD. 2013. Sensory cortex limits cortical maps and drives top-down plasticity in thalamocortical circuits. Nat Neurosci. 16: 1060–1067.

Zembrzycki A, Stocker AM, Leingartner A, Sahara S, Chou SJ, Kalatsky V, May SR, Stryker MP, O'Leary DD. 2015. Genetic mechanisms control the linear scaling between related cortical primary and higher order sensory areas. eLife. 4: e11416.